A Brief Review of the Latest Developments in Hydro-Desulfurization Catalysts Based on Transition Metal Sulfides for the Generation of Diesel with an Extremely Low Level of Sulfur Content

Aymen F. Zwain*, Zaidoon M. Shakor and Bashir Y. Al-Zaidi
Chemical Engineering Department, University of Technology, Baghdad, Iraq.
aymenpetro81@gmail.com*

(Received on 28th December 2023, accepted in revised form 19th September 2024)

Summary: This review paper examines the efficiency of hydro-desulfurization catalysts in removing sulfur compounds from fuels. Specifically, the focus is on bi- and tri-metallic catalysts based on transition metal sulfides (TMS), such as Ni/Co-promoted Mo and W, which effectively eliminate sulfur from challenging compounds present in fuels. The paper is divided into three main sections, each addressing the production of diesel fuel with extremely low sulfur levels using these catalysts. The first section discusses supported catalysts, followed by self-supported or unsupported catalysts, and concludes with a brief overview of theoretical studies. Various factors that can affect the sulfur removal capacity of these catalysts are explored, including the influence of the support material, the use of inorganic and organic additives, and the preparation methods for unsupported catalysts. Based on the review, it is concluded that new experimental and theoretical approaches are necessary to enhance the hydro-desulfurization effectiveness of both supported and unsupported transition metal sulfide catalysts. These advancements are essential to meet the increasingly stringent regulations anticipated for ultra-low sulfur fuels in the future.

Keywords: Hydro-treating; Hydro-desulfurization; Sulfur; Molybdenum; CoMo; NiMo; NiW; CoW

Introduction

The refining processes involved in purifying petroleum products have experienced a substantial increase in production volume due to the continuously rising global fuel consumption. It is projected that gasoline consumption will grow by nearly 1% annually, while the demand for ultra-low sulfur diesel is expected to increase at a rate closer to 2% per year [1, 2]. To meet the expanding fuel demand, refineries are required to handle heavier feeds-tocks derived from petroleum fractions. However, processing these heavier oils presents a complex challenge as it necessitates the application of higher temperature and pressure to effectively remove sulfur from refractory components [2]. Furthermore, the environmental regulations have been adjusted to reach historically lower levels [3], with Europe and the USA imposing increasingly stringent limits on sulfur content in gasoline and diesel. These limits now typically range from 10 to 50 ppm [4]. In addition, there is a global push to achieve "zero sulfur" emissions in the near future [5-7]. The significant reduction in sulfur compounds within diesel and gasoline specifications has led to advancements in more efficient catalysts that can selectively target specific reactions [8]. However, the available information on hydro-desulfurization (HDS) processes and associated catalysts mainly focuses on sulfur removal from lighter petroleum cuts, posing a challenge when aiming for optimal results with heavier feed-stocks. Crude oil sulfur content varies considerably across countries and regions, ranging from 0.10 wt. % for Northern African and Indonesian oil [9] to 6.0 wt. %, as recently recorded for heavy crude oil in Mexican Altamira [10]. Additionally, as global reserves of light crude oil decline, the use of high sulfur heavier oils is becoming more prevalent, as depicted in Figure 1. This emerging demand to process heavier petroleum cuts is currently driving both re-refineries and academic researchers.

Fig. 1: Effects of extremely lower sulfur gas oil producing.

Processing heavy fractions poses notable operational and economic challenges for refineries, primarily because they lack the necessary equipment to handle them [5]. These fractions comprise a more extensive and intricate range of sulfur compounds compared to those typically processed by current HDS units. Previously, a single unit could produce diesel fuel, but now the same unit must produce ultra-low sulfur diesel with less than 10 ppm sulfur content, all while maintaining production levels and achieving an

*To whom all correspondence should be addressed.

improvement in the American Institute of Physics (API) rating for the diesel product [11-13]. To meet these present and future sulfur content limits, highly active catalysts are necessary to selectively remove sulfur from alkyl-substituted di-benzo-thiophene (DBT), like 4,6 dimethyl DBT (4,6-DM-DBT), 4-methyl 6-ethyl DBT (4M,6E-DBT), 4,6 dibutyl DBT (4,6-DP-DBT), and 4,6 dipropyl DBT (4,6-DP-DBT), which are refractory compounds [5,14].

It can be difficult to remove sulfur from compounds that have steric hindrance, as polyaromatics and nitrogen-containing compounds can hinder the process [15]. Overcoming these difficulties involves raising the pressure and temperature conditions in the HDS units. However, this can lead to further complications, such as the gradual deterioration of catalyst stability over time, caused by the separation of active phases and the formation of coke deposits [16]. There are alternative methods available to tackle the challenge of processing heavy fractions, such as renovating or constructing new hydro-treating units. However, these options can be costly [5]. For example, if an HDS unit designed and established in the 1990s for producing gas oil with a sulfur content of 1500 to 350 ppm needs to be upgraded to produce ultra-low sulfur diesel with less than 10 ppm sulfur and achieve an increasing API in the diesel cut, a revamp would be necessary. According to the Environmental Protection Agency, the cost of installing a modern HDS unit at a refinery to produce ultra-low sulfur diesel with a sulfur content of 15 ppm or less is estimated to be twice the cost of producing low sulfur diesel with a sulfur content of 500 ppm [17, 18].

The extensive body of literature on hydro-desulfurization catalysts for ultra-low sulfur diesel production encompasses diverse research approaches pursued by specific investigation groups [19]. Researchers have utilized advanced techniques to investigate the structure, surface area, dispersal state, promotion state, morphology state, and activity of catalysts involved in the hydro-desulfurization process [19,20]. While it is difficult to categorize all the relevant literature, this review will be organized into three main categories: catalysts with supports, non-supported catalysts, and theoretical studies. Our review primarily focuses on the preparation of catalysts for diesel hydro-desulfurization, encompassing both non-supported and supported catalysts. These catalysts are designed to reduce the presence of sulfur compounds in diesel and produce a purified gasoil fraction. The objective of these methods is to decrease sulfur quantity in the diesel cut and/or modify the properties of sulfur compounds to facilitate their removal, while also maintaining a desirable octane number for the diesel. However, it is crucial to strike a balance between sulfur removal and minimizing the loss of olefin saturation, posing a significant challenge. In conclusion, this review will aid researchers in selecting the most effective catalyst conditions, specifications, and types that ensure high-quality sulfur removal.

Supported Catalysts in HDS

The Function of Active Sulfide Phase Support

The activities of catalysts, morphology, and dispersion of the prepared catalysts are generally affected by nature of the support used [21, 22]. Conventional alumina, which is commonly used as a support, is not completely inert under reaction conditions and it is possible that the immigration of active promoters like Co or Ni to the external surface may occur, resulting in the formation of sub-surface spinels [23], or promoting isomerization processes based upon the acidic properties for those ions. Topsoe *et al*. reported that eliminating or significantly decreasing the interplay betwixt the CoMoS phases as well as the alumina support could result in modern sulfide structures with more intrinsic activity [24, 25]. This led to propose a CoMoS phase type II structure with less support interaction. Ever since, a significant amount of research has been carried out to modify the interaction between the support and activated phases. It is widely acknowledged that catalysts used for diverse oil fractions should have slight variations in their interactions between metal and support. Wherefore, the dispersion of active phases over alumina plays a crucial role in determining the catalyst's activities, selectivity, and stabilities (refer to Fig. 2) [16].

The importance of understanding The function of the support in hydro-treating catalysts has been widely recognized and investigated. Several studies have focused on the dispersion state, stacking state, as well as length of MoS_2 or WS_2 slabs, as well as the manner in which the metal sulfurets are attached to the surface of the support [26]. The morphology and orientation of MoS_2-based catalysts have been found to strongly influence their catalytic performance, with the preferred bonding depending on the support used [27]. For instance, gamma alumina typically favors bonding by the basal planes (111) and (100), As demonstrated by Bara *et al*., they exhibit moderate to weak interactions with MoS_2 structures. [28]. In contrast, bonding on the (110) plane results in oxide particles that are well dispersed and oriented, with a robust metal-support interaction. The bonding of MoS_2 clusters to the surface of TiO_2 anatase by the edges plane was demonstrated by Sakashita *et al*. [29]. Transmission electron micrographs presented in Figure 3 illustrate the (002) planes of MoS_2 clusters, which have an interplanar spacing of 0.6 nm

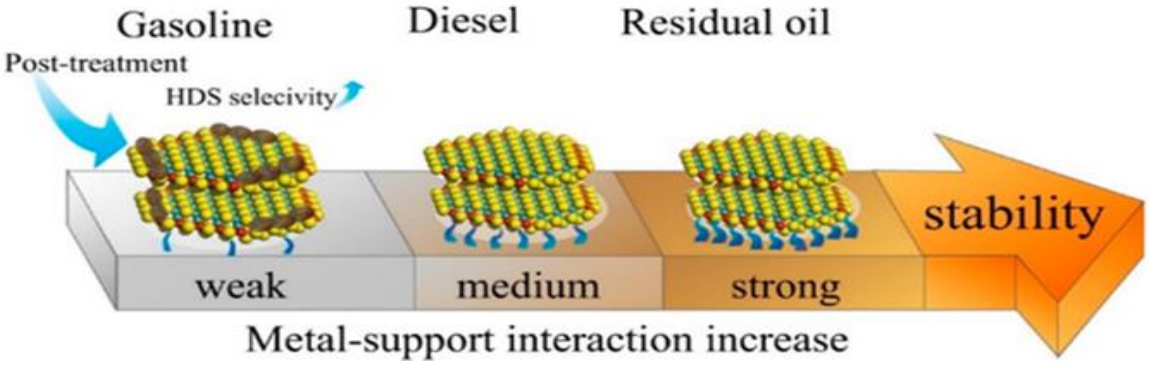

Fig. 2: The various metal-supports interacting in hydro-treating catalysts [16].

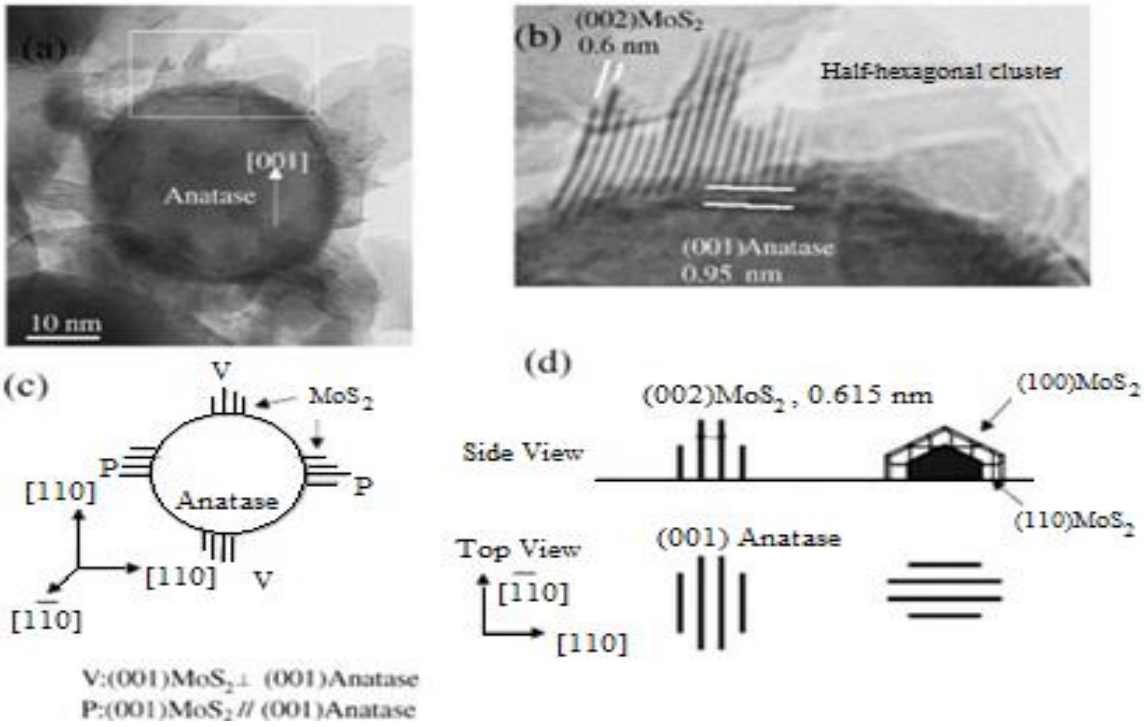

Fig. 3: (a & b) The transmission electron micrographs (TEM) and schematic diagrams (c,d) Illustrate MoS_2 clusters / TiO_2 anatase powders [29].

Several years after, it was confirmed by Arrouve *et al*. through density functional theory (DFT) computations that the anatase surfaces has the capability to increase both perpendicular and tilted alignments of the p MoS_2 clusters, owing to epitaxial growthing. Additionally, they suggested that the (110) hydroxylated alumina plane/surface could enable a slab inclind orientation p due to the pliability of its hydroxyl group [30-32].

In a recent discussion, Berhault pointed out that the influences on catalytic behavior include the particle size along the MoS_2 particles axis and the ratio of edge-basal plane [33]. His group's research revealed that active sites could also be formed on basal planes when the slabs possess some degree of bending [34]. However, observing the entire effective phase and isolating the curvature effects remains a significant defiance. As Berhaulte noted the state of disorder in molybdenum sulfide, its dissipation, and the limited visibility of only 10.0% of the active phase via transmission electron microscopy because of slab orientation all participate to this difficulty. In a recent publication, Díaz de León *et al.* examined the influence of the support on p NiW p catalysts and discovered the presence p of slabs with some degree

of bending in nearly all samples tested using highly-resolution transmission electrons microscopy (HRTEM) [4]. The bending was more prominently detected in NiW catalysts which prepared over mixed oxides [35].

They suggested that the interaction of metal-supports p can be controlled by replacing the p carrier, while this interaction is immediately reflected in the p slab length. Notably, they discovered that the jumbled oxides of ZrO_2-TiO_2 (ZT) as well as Al_2O_3-TiO_2 (AT) exhibited the topmost activities amongst the p series p. The findings they obtained of DFT demonstrated that the p promoted slabs have a tendency to bend due to the interaction p with p the support, this leads to a reordering of charges that causes a reduction in p crystallization and the formation of flaws with significant hydrogenation ability throughout the slabs at the flexion points [36] p, as previously highlighted by Shimad and his team [36]. In the present context, Afanasie lastly generated blank metal sulfide nanoparticles to investigate the effect of slab curvature (as shown in Figure 4) [35]. A considerable quantity of fault in the hollow MoS_2 nano-spheres were detected by him, resulting from plane dislocations (002) near the junction points. His results provided substantial proof of the contributions of the curved basal surface of the slab to the catalytic activity. Additionally, his proposal was that for supports with similar chemical properties, MoS_2 particles with greater curvature may have an advantages over least curved ones. [37].

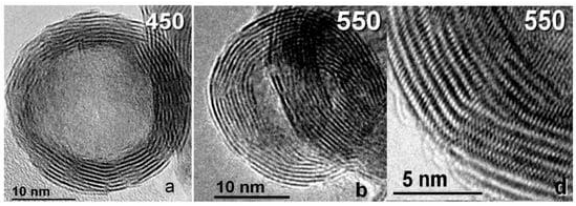

Fig. 4: The HRTEM images of the hollow spheres, which were designed and adapted by P. Afanasiev [37].

A Distinct Method: Using Support Mixed Oxides

As previously mentioned, researchers have explored various approaches to modulating the metal-support interaction, this encompasses the utilization of crystallographic phases other than gamma alumina [60], as well as non-traditional single metal (MS) oxides like Ti [26, 61-67], Zr [26, 63-66, 68, 69], Sì [22, 26, 70-72], or Ga. [72, 73]. However, more newly, to leverage the individual properties of single metal oxides and to address their limitations, research has been conducted on mixed oxide material consisted of two elements, like Al_2O_3-Ga_2O_3 [71, 72], Al_2O_3-TiO_2 [3, 74-79], ZrO_2-TiO_2 [35, 80, 81], Al_2O_3-ZrO_2 [82-84], MgO-TiO_2 [85], Al_2O_3-MgO [78, 86], Mn-Al_2O_3 [87-89] and Al_2O_3/zeolites [90], amongst others, for preparing HDS catalysts. As anticipated, in various scenarios, catalysts supported on mixed oxides showed higher activity compared to those supported upon alumina. Changes in the morphology parameters, like the length and MoS_2 slabs accumulation, demonstrate that interplaying can be modified. Several researchers have also noted significant variations in support characteristics, including surface acidities, area of surface, surface potential, properties of electronic, and more.

However, there is still no clear understanding of the relationship between the structure and activity of these mixed oxide supports, and the precise makeup of each support used in the mixed oxide can influence the resulting catalytic properties. Previous studies have shown that Mo supported on Al/Ti = 1 and Ti/(Ti + Zr) = 0.79 gave the topmost activity for hydrocracking process and upgrading coal-derive liquids [91]. Meanwhile, for the hydro-desulfurization of DBT, sundry studies have reported the highest activity when using Al/Ti = 2 in materials prepared using the sol-gel method [4, 35, 74, 77].

The activity results of catalysts are influenced by the precursors and methodology used for mixing [92,93]. Our research group recently investigated to examine how the sulfide cluster interacts with surfaces, the impact of the support on NiW catalysts was investigated [4,35]. When a catalyst is made, metal–O–Ms connections are typically formed (Ms being the metal in the support), which are fractured and converted into Mo-S-Ms bonds during sulfiding. However, some Mo–O –Ms bonds may persist at the periphery of MoS_2 slabs [94]. DFT calculations can be used to redefine the bonding between the metal sulfide layer and the support after the formation of Mo-S bonds. Our findings suggest that Ti-supports exhibit clear orientation effects on metal sulphide slabs, though mixed oxides demonstrate greater affinity towards Al or Zr than Ti. Consequently, when clusters avert certain surface atoms, they tend to bend, a phenomenon that warrants further examination in light of the recent discoveries as previously discussed in above section.

A description the preparation of Ultra-Low Sulfur Diesel catalysts

Typically, supported catalysts in industry are prepared by impregnating metal precursors over hotter

alumina pellet using the incipient wetness method. Additives, whether organic or inorganic, can be incorporated into Al_2O_3-based catalysts to modulate their activity. As a result, the additives hinder the migration effect, leading to an augmented involvement of promoter-atoms in the creation of the nonstoichiometric CoMoS phase via the S-edges of MoS_2 [73]. These additives prevent migration, thereby increasing promoter atoms are involved in creating the non-stoichiometric CoMoS phases across the S-edges of MoS_2 [72]. In the preparation of catalysts, the metal hydroxide species present in the mother solutions (at a specific concentration and pH) could potentially include cationic entities, such as the $[Ni(H_2O)_6]^{2+}$ species [74]. Thus, the concentration, degree of temperature, and the carrier surface for catalyst preparation can be cationic, or anionic, such as MoO_4^{2-}, p [23, 75], $W_6O_{21}^{6-}$ and $HW_6O_{21}^{5-}$species p p [76], at the same-self of pH value. At a pH of about 8, alumina has p a zero-point p of charge (ZPC), and its surface is negatively charged above this value and positively charged below it [75]. According to Diaze de Leone *et al*., a modification in the surfaces potential can potentially alter the deposited species on the surface. Their Raman spectroscopy findings indicated a variation in the ratio of terminal (Op = Wp = Op + Wp = Op) bonds to internal Wp–Op–Wp bonds, which was dependent upon the surfaces potential of the supporting materials [75, 76]. Vazque-Garridoe *et al*. connected the discrepancies in the potential of Z type of their supports (4.9 for Al_2O_3-TiO_2 and 9.0 for Al_2O_3-MgO) to variances in the Mo oxides surface species [57].

Organic Additives

As previously mentioned, active phase precursors such as molybdenum, or tungsten promoter atoms like Co or Ni, and additives are often included in the preparation of hydro-desulfurization catalysts. However, achieving maximum activity relies on optimizing the formation for each of CoMoS, NiMoS, or NiWS mixed sulphide phases. Chelating agents have proved to be a useful tool in the synthesis of HDS catalysts with a high level of activity. These agents first form combination with the cobalt, nickel, molybdenum, or tungsten precursors, modifying their coordinate sphere and inhibiting the creation of isolated ions on the support surface; this increases promoter ion participation in the synthesis of nonstoichiometric Co(Ni)Mo(W)S phases. Chelating drugs also have the ability to slow the sulfidation process, which has been demonstrated to inhibit the segregation of thermodynamically steady Co or Ni sulfides (Co_9S_8 or Ni_3S_2) [76-78]. While it is well recognized that cobalt oxides sulphidation occurs at a lower temp than tungsten oxide sulfidation, there have been few investigations on the segregation impact that occurs midst the sulfide processes, particularly for Co-W sulphide catalysts [79, 80]. A substantial amount of stable Co_9S_8 may be produced at a temperature of 473 K, as shown by Kishan and Escobar *et al*. They also found that once WS_2 is generated, NiSx particle re-dispersed to create the NiWS phases [80, 81]. CoSx particles, on the other hand, continue to create more Co_9S_8 than the CoWS phase.

Some authors have proposed that employing chelating agents might offer a solution to this issue. Kishan *et al*. effectively employed 1,2-cyclohexanediamine-N,N,N,N-tetraacetic acid (CyDTA) and triethylene-tetraaminehexaacetic acid (TTHA) in the impregnation process, resulting in approximately 2.4 times higher activity for CoW catalysts prepared with TTHA compared to those prepared without chelating agents [82]. The preparation of $NiMoP/Al_2O_3$ using saccharide (SA) as an organic additive during concurrent impregnation has been reported [83]. The addition of a small amount of SA improved the dispersal of metallic species, increased the sulfurability of Ni oxide species, and enhanced catalytic activity. However, a higher SA content led to increased carbon content, resulting in intense blockage of active places. The use of ethylenediaminetetraacetic acids (EDTA) has also been reported to have favorable effects, promoting the formatting of active phase p and increasing activity p [77, p 84- 86]. Lately, hydrocarboxylic acids, particularly citric acid (CA), have been shown to be effective in preparing promoted catalysts p such as NiMo, CoMo, or NiW p systems, because of their outstanding solubility and low cost [87]. Several studies have suggested that CA can enhance the dispersion of Mo (W) [88-92], altering the morphology of the MoS_2 slabs has been achieved in previous studies [93,94]. alter the drastic metal supports interaction [73,89,95-97], and delay the sulfidation practicability [73]. Similarly, it is generally agreed upon that citric acid enhances the promoting influence of Co or Ni atoms, thereby augmenting the contribution of the promotion atom in creating the Co(Ni)-Mo-(W)-S mixed phase.

The morphology of active species can also be affected by the pH of the impregnation solutions, as previously mentioned. Several studies by Valencia D. *et al*. demonstrated that the pH level of the impregnation solution plays a crucial role in determining the activity and selectivity of NiMo catalysts, especially when combined with CA [98-100]. The authors also reported that increasing the

amount of CA meantime synthesis improved the NiMo catalysts in the direct HDS pathway. Additionally, Castilloe-Villalo *et al*. reported that the addition of CA changed the MoS_2 crystallites morphology by increasing the formation of Mo-S sites [101]. Chen K. *et al*. simultaneously published similar results, demonstrating that CA aided in the formation of the S-edge of MoS_2 slabs and progressively transformed their shape from a slightly truncated triangle with mainly as seen in Figure 5., the M-edges were transformed into a hexagon shape, maintaining a similar size proportion of M-edges and S-edges.

Suarez-Toriello *et al*. demonstrated that the incorporation of CA could prevent at higher temperatures, excessive interactions between the metal and the support may occur, which can delay the reduction of nickel by inducing isolation of impregnated metal species. The authors discovered that CA inclusion hindered the formatting of unsolvable nickel species as well as instead of produced dissoluble Ni-Cit species. Their findings from XPS and activity tests indicate that this leverage leads to an increase in Ni's involvement in the forming of the non-stoichiometric NiWS phases [74].

The operational conditions and the quality of the liquid feed are among the factors that strongly affect the lifespan of a catalyst in an industrial hydro-treater. Over time, coke deposition tends to cause deactivation of HDS catalysts, metal poisoning, sintering, and other pollutants [102]. Dufresne has it was suggested that certain oxygen components can serve as metal dispersal agents when reactivating a decoked catalyst [102]. In this context, chelating agents have shown promising results in controlling the regeneration of spent catalysts. Bui *et al*. used maleic acid to regenerate CoMo catalysts [103]. They found it has been suggested that this chelating agent can efficiently extract Co from $CoMoO_4$ species and forming a complex of maleate with cobalt. The release is caused by this complex Co after temp. 300°C, which promotes the redeposition of MoS_2 slabs and increases activity.

Han *et al*. [104] treated spent CoMo catalysts with CA, Ethylene Glycol (EG), tri-ethylene glycol (TEG), thioglycolic acid (TGA), and dimethylsulfoxide (DMSO), finding comparable results as Berhault and his team [10p3]. The researchers observed that using CA, EG, TEG, or TGA nearly entirely restored the catalytic activities by allowing for the re-dispersion of p activated metals, hence facilitating the creation of a new, strongly promoted p active p CoMoS phase. The authors also suggested MoO_4^{2-} or β-$CoMoO_4$ polymolybdate species can be effectively generated from these species. Moreover, the addition of CA can aid in the recovery of Co^{2+} ions from the sub-superficial $CoAl_2O_4$ spinels, thus promoting the formation of more CoMoS sites.

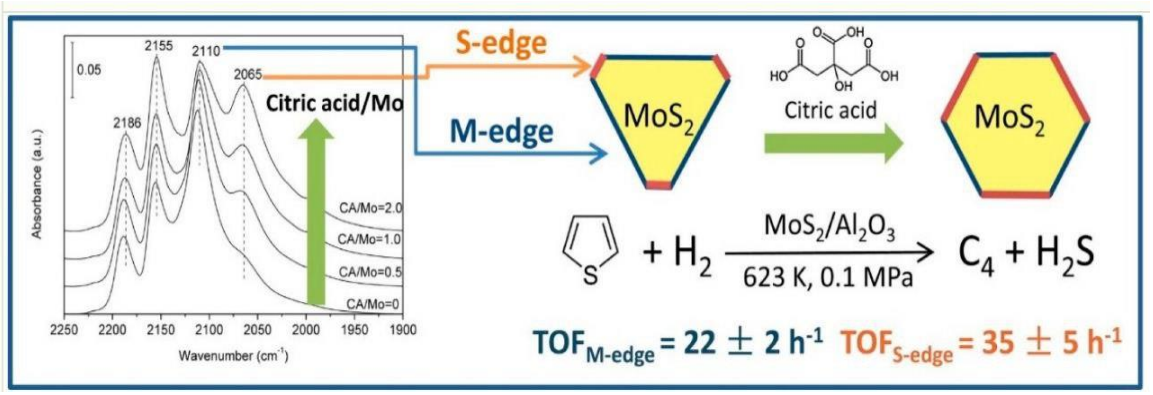

Fig. 5: The impact of citric acid on the morphology of MoS_2 slabs [94].

Inorganic Additives

As previously discussed, chelating agents are often utilized to avoid losing of promoter atoms located in sub-surface supports layers. This phenomenon occurs when hydroxide cations of Ni atom (or Co) directly interact with under-coordinated cations at the outermost layers of the metal oxide exterior surface, in octahedral or tetrahedral sites. This migration leads to the loss of some of the promotion of catalysts with a charged promoter in the formatting of sub-surface spinels.

Admixtures such as F [10 5, 107], Mg [106-11 0], B [111-116], P [85,117-119], or Ga [76, 120- 124] have been founded to effectively address immigration phenomena and enhance stability while reducing the interaction between the catalyst's active phase and the support material. However, it is important to carefully consider other factors such as activity and selectivity as changes in surfaces and texture properties can occur, and in many cases, an increase in the concentration of additives may result in a reduction in activity [76,118].

Changes in surface acidities are typically reported as a result of introducing additives like F [105,107], Mg [107-112], B [113-115], P [85,117-119], or Ga [75,120-124]. For instance, B, F, Mg, and Ga adjust the Bronsted acidities, causing changes in the property of electronic of MoS_2 and CoMoS sites, and affecting the morphological property of the sulfide phases to varying degrees [106-125]. Ga, in particular, when used as alumina support additives, the modification of the dispersion process and increased promoting of the effective phase to nearly the Upper limit theoretical Ni promotion ratio alters the general morphology of WS_2 slabs [120]. This suggests that the presence of $GaAl_2O_4$ on the surface not only alters the surface potential relative to the alumina in its initial or primary form, but also prevents migration of Ni within the catalyst, this results in a substantial augmentation in the amount of Ni present in octahedral species ($Nioct^{2+}$) that promote the active phase [126]. Hani and others discovered that the insertion of F at the system of MoS_2/Al_2O_3 has a significant leverage on the Bronsted acidity [107]. The authors suggested that the Bronsted sites have an interaction with the active phases present in the surrounding area, inducing an electron-deficient state that increases the formation of p coordinatively unsaturated sites and raises amplitude of hydrogenation process.

Furthermore, it is expected that the hydrogenation pathway will occur via π-bonds because of the hindrance caused by the presence of alkyl substituents. The presence of what is commonly referred to as BRIM sites has been associated with an increase in hydrogenation process capacity [127]. Consequently, it may be claimed that the presence of chemicals increases the domestic metallic features of Ni-Mo(W)-S edge sites in the phases adjacent to these additives of metals. Changes in particles size can also impact the metallic nature of NiWS edges [29, 30]. Additionally, the addition of additives can enhance the activated phase dispersal. Hence, the modification in the size of slab alone could account for changes in selectivity.

The ability of hydro-desulfurization supported catalysts to function effectively is influenced by various factors, such as the active component, support type, inorganic-organic additive concentration, pH value of the impregnating solutions, metal-supported interacting, promoter type and amount, slab length-stacks No., and sulfidation temp. and time. Moreover, non-organic-inorganic additives can enhance thermal stability, regulate metal-supports interactions, improve metal sulfide dispersion, acidity value, and generate coordinately non-saturated sites in the catalysts species. By considering all over these factors, it is feasible to design a catalyst that can confidently produce ultra-low sulfur fuels.

Structure-Activity Relationship of Unsupported Hydro-desulfurization Catalysts

In lastly years, it has been a growing interest in unsupported catalysts because their higher activity compared to supported catalysts, which is approximately 2.5-3 times higher. The refining industry has also been compelled to produce ultra-low sulfur fuels due to strict environmental regulations. These catalysts can be used as a whole or as a layer (20 to 30% reactor bed) in the reactors utilized for the production of ulta low sulfur diesel in the industry. This part focuses on relation between structure and activities of non-supported catalysts. On the contrary, supported catalysts, self-supported catalysts do not exhibit any metal support interactions, either strong or weak. However, the activity of the catalysts is influenced by the length and stacking of the metal sulfide slabs, which are determined by the procedure for synthesizing the catalysts. Therefore, the method of catalyst synthesis is crucial, and this section is categorized into two subsections: the first topic pertains to the metal sulfides direct synthesis via the decomposing approach, whereas the second topic focuses on the synthesis of metal oxide precursors that are subsequently sulfidized in-situ/ex-situ.

Thiosalts Decomposition

This section is dedicated before discussing the structure-activity relationship of both bulk MoS_2 catalysts with and without promotion, which are produced by decomposing precursors like thiol-salts [128-131], alkyl-contain of salts [130-134], oxythiol-salts [135,136], as well as others. Numerous factors have been identified in the literature as the association of support properties with the impact of alkyl-containing compounds on catalyst performance and their influence on the selectivity path (hydrogenation (HYD) or direct desulfurization (DDS)) and HDS activity. These include carbon effects, promoter effects, transition metal sulfides, the temperature at which catalysts are activated, using of gas activating, and manufacturing methods.

The effectiveness of catalysts that were synthesized by decomposition in HDS is determined by several factors such as the amount of promoter, the temperature at which it is prepared, and the type of gas (hydrogen or nitrogen) used for activation. These factors can also impact the characteristics of the catalysts such as long of slabs, No. of layers, as well as slab orientation. For instance, catalysts containing nickel (NiMo or NiW) promoted under high temperature and hydrogen environment have been found to exhibit high activity with stumpy slab lengths and low stacking degrees. Iwata *et al.* [34] and Araki *et al*. [37] have reported that catalysts with low stacking degree and curved slabs also exhibit high activity the existence of imperfections in the slabs, as explained in Section 2.1, resulted in a smaller size of MoS_2 slabs and higher activity for CoMo catalysts which activated with a hydrogen gas via the DDS route. In contrast, CoMo catalysts activated under a nitrogen environment exhibited larger stacking numbers [129].

Unsupported catalysts often have lower surface areas, least slab dispersion, and lengthy slab lengths, which can limit their catalytic performance. To address these issues and enhance performance, some of researches groups have employed organically surfactants spices [136] and alkyl-precursors [132-136] that act as internal templates to enhance the spread of metals sulfide slabs and maximize the surface area during catalyst synthesis, Acuñ *et al*. developed catalysts (CoMoW) with varying carbon atom chains length from C_1 into C_3 and found that increasing the alkyl-chains length led to a significant increase in organic carbon content and BET surface area, but had little effect on catalytic activity [132]. The authors noted the primary limitation of compounds containing alkyl groups precursors was the generation of char while undergoing decomposition, which blocked active sites and negatively impacted HDS process activity. They also observed that increasing the alkyl-chains length decreased slab length but did not affect stacking degree. In contrast, Armenta *et al.* found that using longer carbon chains (C_{12} to C_{18}) for the same tri-metallic catalyst (CoMoW) resulted in the formation of sulfur carbide, which acted as a dispersing agent and improved HDS activity [133]. The researchers noted that the dominant reaction pathway was the DDS route, which relied contingent on the amount of carbon present in the resulting catalysts. Similarly, Romer *et al*. declared that the MoS_2 catalysts activity was proportionate to length of alkyl chain up to a certain range, beyond which carbon acted as a poison by covering active sites [134].

Additionally, the preferred mechanism for catalysts was through the hydrogenation pathway. The extent of metal oxide sulfidation, which governs the mechanism of HYD or DDS, as well as the catalyst's ability to withstand heterocyclic compounds present in the feed-stock, is significantly influenced by the catalyst's type of promoter and the amount of loading can have an impact, according to reference [136]. Metal sulfides such as MoS_2 as well as WS_2 were known for their effectiveness in HDS, but the un-promoted catalyst's HDS performance is dependent on the feed type. Olives *et al.*'s research on hydrogen index and hydro-desulfurization of model compounds indicated that MoS_2 was highly active in model compounds but performed poorly in real feed due to substantial (hydrogenation pathway) and environmental state (organo-nitrogen tolerance) factors [137]. The addition of Co to MoS_2 significantly improved its activity in the real feed-stock, emphasizing the significance of the promoters. Unsupported catalysts of MoS_2 have been promoted using assorted promoters like Co, Ni, or Fe, as reported in reference [138]. The authors found that Ni had a higher sulfidation degree, which is consistent with Le *et al.*'s results for NiW unsupported catalysts [135]. In contrast, Yi *et al*. it was found that an increase in the Ni content of the catalyst led to a decrease in the cumulation of Mo/WS_2, that resulted in low effectiveness [139].

In addition, the amount of promoter content plays a significant role in determining the catalyst's mechanism, whether the reactions proceed during the HYD or DDS pathway. Bocarando *et al.* noted that high promoter loadings increase HYD route, while low promoter loadings increase DDS [140]. Zepeda *et al*. reported that metal additives like Ga can create sites in the catalyst that are coordinative unsaturated [141].

In addition, certain scholars have analyzed energies of the bond between metal and sulfur and their influence on stoichiometric sulfur situated at the edges of MoS_2 slabs [142,143]. In a study by Daudin *et al*. [142], various transition metal sulfides were investigated, and a relationship between HDS/HYD ratio selectivity and energies of the bond between them was observed, as depicted in Fig. 6. The authors suggested three scenarios: (1) low and high (2) sulfur-metal bonds energy showed a high level of activity for hydrogenation process mechanism, while moderate (3) metal-sulfur bond energies resulted in a significant rise in DDS, this led to the highest ratio of HDS to HYD among the available all the systems analyzed. Furthermore, the researchers discovered that their experimental data was an excellent match for Langmuir-Hinshelwood kinetics. They postulated that Me-S (sulfur in metal) species and unoccupied metallic sites facilitated the disintegration of H_2S as well as H_2, whereas organosulfur molecules in competitive adsorption and alkenes occurred exclusively upon metallic sites. According to Afanasie *et al*. [143], the stoichiometric sulfur atom (S_2^{2-}) found at the non-supported MoS_2 edges slabs is crucial to the catalytic activity. The interaction of S_2^{2-} species with hydrogen generates -SH groups, which strongly affect the behavior of the catalysts. Catalysts exhibiting this effect control The HDS process using the HYD pathway. When -SH groups are present at the edges of MoS_2 slabs, the affinity of nickel and cobalt ions towards them is lower than in their absence.

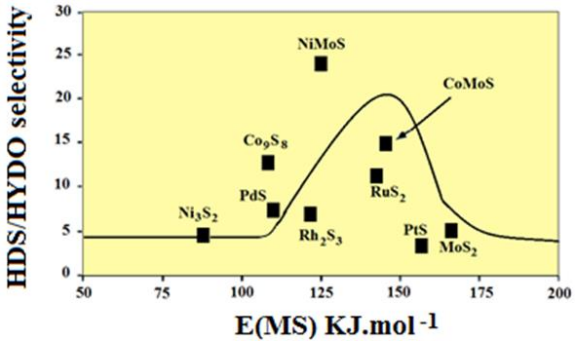

Fig. 6: The hydro-desulfurization selectivity a comparison of experimental outcomes and a kinetic model (represented by a black line) at a temperature of 250 °C, pressure of 20 bar, and H_2/feed Ratio of 360 L/L, based on the energies of sulfur-metal bonds (E(MS)) [142].

Sulfidation after Oxides

Template-Free Method

When considering catalysts that are prepared through a method devoid of templates, the oxides catalyst was subjected to a thermic sulfidation processes, three synthesis procedures were discussed: (a) the use of layered-double hydroxide molecules [144–147]; (b) the hydro-thermally way [148–152]; and (c the precipitation methods [152-154]. Hydroxides with double layer serve as both precursors as well as structural template for the synthetic HDS catalysts species [147]. The activity of LDH-derived catalysts is contingent on multiple factors, including the geometric arrangement of metals ions in the hexavalent state (whether in tetrahedral coordination or octahedral) [144], the precursor oxides surface area, content of promoters, activation temperatures, and others. Similar traits were noted between catalysts obtained or extracted from LDHs and thiosalts. Compared to the ones obtained from thiosalts, the activation temp. of catalysts obtained or extracted from LDHs containing W (as mentioned in reference 146) are relatively high. Moreover, Coelho *et al*. did not find any correlation between the activity of LDH-derived catalysts and characteristics like Mo/Al ratio or surface area [145].

The hydrothermal method was also used to synthesize unsupported catalysts with high surface areas. The catalytic activities of these catalysts strongly depends on their temperature of the invigorate, which is influenced by their catalytic properties, such as crystalline nature, basal plane defects, size-shape, and conglomerate of metals sulfides [148, 149]. Studies by Yini *et al*. [152] and Zhang *et al*. [149] demonstrated that rising the sulfidation temp. led to the agglomeration of $Ni3S_2$ and MoS_2/WS_2 nanoparticles, resulting in longer MoS_2/WS_2 slabs with a curved shape [148, 149]. Furthermore, defects on the basal planes were reported to act as sites that exhibit high activity in the HDS process reactions [2.1], and the existence of Lewis's acidic sites was found to cause de-alkylation and isomerization reactions in alkyl-substituted DBTs [150, 151]. The researchers discovered that enhancing the catalytic properties is linked to the degree of sulfidation increase and the efficient dispersion of the active components. Furthermore, they established a clear association between the conversion of DBT and the presence of sulfur weakly bonded to the catalyst surface (Figure 7).

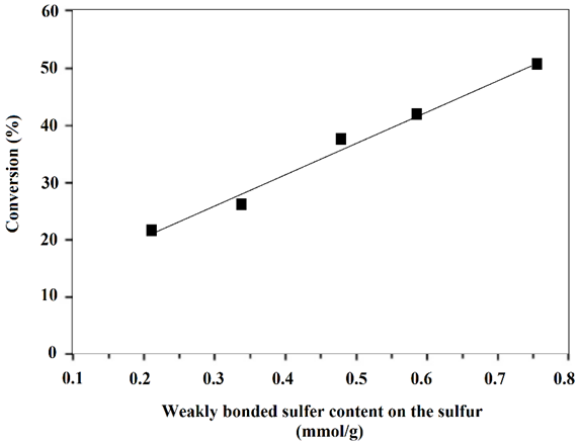

Fig. 7: The correlation betwixt the conversion of DBT and the S content weakly bound to the catalyst [154].

Template Method

The use of organic templates is another technique to achieve high surface areas and improve dispersion. This section discusses the hydro-desulfurization activity of catalysts produced through the utilization of diverse organic templates, like polyethylene polyethylene glycol [152–155], polivinylpyrrolidone (PVP) [156], pluronic 123 (P-123) [157], tetrabutylammonium bromide [158], or biotemplates [159]. Templates can enhance morphology, thermal stabilities, as well as the formation of active NiMoS/CoMoS phases [152]. Unsupported HDS catalysts have assorted morphologies, such as resembling a belt [153], fullerene-like [154], and resembling a core-shell configuration [155] the particles which possessing a higher number of active sites. The morphology state and property of active phases of the catalyst are determined by the quantity of surfactant utilized during synthesis. Liu *et al*. [156] reported it can be concluded that using a small quantity of surfactant (PVP) leads to the production of a high surface area NiMoS phase with significant activity and the -$NiMoO_4$ phase is preferred. Compared to supported catalysts, unsupported catalysts typically have longer slab lengths, which seems to exert a stronger influence on HDS activity compared to the number of layers stacked [153, 158]. The catalyst synthesized using surfactants like cellulosic fibers showed a positive effect of carbon. The catalyst produced by thermally decomposing alkyl-contained precursors (as illustrated in Section 3 .2.1) has similarities. Certain experimental results suggest that, rather than an increase in stacking number, an increasing slab length is more crucial in order to achieving high HDS process selectivity [153,160]. As previously discussed, promoters encourage the development of the active phase. In fact, the NbS_2 catalyst promoted by copper displayed greater activity per mass than molybdenum sulfide [157].

Unsupported catalysts are known to have higher activity than supported ones, but they also have drawbacks like low surface area and catalyst sintering. Unsupported catalysts synthesized from thio-salts are expensive and cannot be scaled up, and their promoters can oxidize when exposed to the environment. To address these issues, precipitation way and hydro-thermally method are always eco-friendlier options for synthesizing unsupported catalysts. The activity of these catalysts can be improved by increasing their surface area and dispersion, which depends on various factors such as the catalyst's preparation method, precursors, and organic surfactants used. The degree of sulfidation, metal sulfide slab shape, size, length, and orientation are also important in determining the catalyst's activity. Shorter slab lengths with minimum of two slabs in the stack and larger Mo edges in the slabs are ideal for achieving high hydro-desulfurization activity.

Theoretical Studies

Academic studies, specifically those utilizing DFT computations or analyses, have significantly contributed to a comprehension of the chemical and physical characteristics of materials containing MoS_2, and their correlation with experimental observations. According to the theoretical findings, corpus 2H-MoS_2 is a substance that exhibits band gaps that can be either direct or indirect that align very closely with the experimentally reported values [159-161]. However, it is also predicted that the chemical, optical, and electronic properties of this material can be modified by introducing transition metal doping or applying pressure, leading to the development of intriguing new technological applications [162-164]. In addition, there is a vast range of possibilities available when reducing the dimensions of these materials, as it enables band-gap engineering [165-176] and results in the acquisition of novel magnetic properties [177-179].

Theoretical results have demonstrated that Mo-edges in MoS_2 slabs are more effective for catalysis than S-edges when both bares Mo- and S-edges are exposed [180-183]. This has been further supported by recent research showing that the primary reaction route for thiophenes hydro-desulfurization

takes place across the Mo-edges, while the activation of Mo-S bonded edges relies on the temperature [184].

In addition, Yang *et al*. [185] identified an optimal cluster size, $Mo_{27}Sx$, for the purpose of conducting catalytic investigations. This cluster size allows for adsorption of various sulfur compounds on different active sites of both S- and Mo-edges [186]. Sun *et al*. [187] used DFT studies to observe the molecular behavior of the 4,6-DMDBT, which switches involving adsorption on edge and rim sites via both π and σ interactions. They discovered that the formation of vacancies is not ideal under HDS conditions. In addition, they used scanning tunnelling microscopy (STM) depiction to demonstrate that the adsorption of the 4,6-DMDBT molecule via the DDS route can only occur on the vacancy located at the edge or corner of the S-shaped curve within the CoMoS nanocluster (as shown in Figure 8).

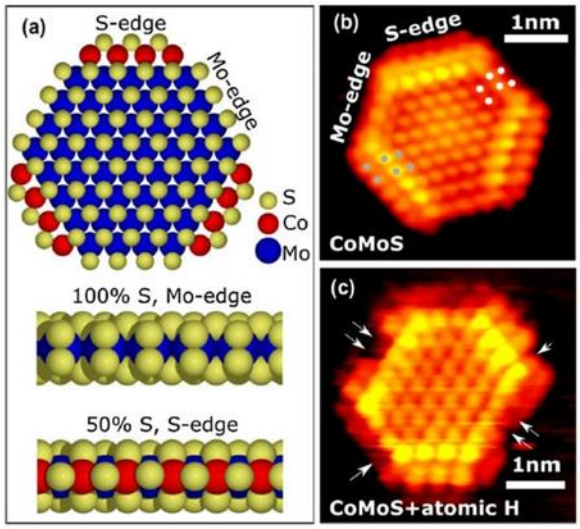

Fig. 8: (a) The molybdenum and sulfur edges in the catalyst of CoMoS, (b) Scanning tunneled microscopy photos of the CoMoS nanoclusters, and (c) The creation of vacancy at the center of the Mo edges instead of the corner upon exposure to H_2 [187].

Previous studies dealing with tri-metallic catalysts consisting of Co(Ni)Mo components, especially during HDS conditions, indicates that Ni is more inclined to integrate with the Mo-edge, whereas Co has a preference for the S-edge in periodical slab of model under typically sulfidation process conditions [188]. However, at the nanoscale and in theory, it is possible for Co-Mo or Ni-Mo edges to coexist, even though during HDS conditions, the slabs tend to adopt a hexagonal shape where the Me-edge is partly adorned with Co and Ni, whereas the S-edge may have partial Ni decoration [189]. Therefore, the participation of Ni atom or Co atom that used in the process of promotion is a decisive factor in enhancing the selectivity ratio of HDS over HYD [190].

Furthermore, we also confirmed that the morphology of the support can have a significant impact on catalytic activity of these materials, which could further influence the approach invoked for the design of these materials. [191,192]. To understood the clusters/supports interacting, one of the earliest theoretical studies focused on the divergence in catalytic activities observed between CoMoS structures of Type-I and Type-II that are backed by alumina [193,194]. The reason for the feeble interaction between Types-II CoMoS structures and the supports could be the fact that generating vacancies in such a scenario involves a process that requires a substantial input of energy that significantly reduces S linkages.

While theoretical studies can contribute significantly to our understanding of the mechanisms underlying catalytic processes and the design of improved catalysts, it remains unclear how the property of catalysts species are influenced by various the stability of catalytic supports when exposed to various thermodynamics conditions. Nevertheless, such studies can inform the development of new strategies aimed at improving catalyst performance, enhancing reaction stability, and extending catalyst lifetime. Characterisation results revealed that by co-impregnation, the dispersion of the Mo phase was significantly increased due to the presence of Ni and, on the other hand, more Ni stay together to Mo on the external surface of the clay, favouring thus the formation of Ni-Mo–O interaction species, precursors of the "Ni-Mo–S" active phase.

Kinetics and Mechanism of Transition Metal Sulfides

Hydrotreatment applications for the removal of heteroatoms, such as sulfur from oil feedstock, represent a significant process in the petroleum refining industry. Despite the extensive application of hydrotreating catalysts based on transition metal sulfides (TMS) and considerable research over recent decades, many aspects of HDS remain not fully understood.

For example, the reaction mechanism for the HDS of the commonly used model compound thiophene is still debated. Early proposals suggested that thiophene desulfurization occurs through double β-hydride elimination followed by rapid hydrogenation of adsorbed diacetylene to 1,3-

butadiene [195]. Alternatively, Lipsch and Schuit proposed that the carbon-sulfur bonds undergo hydrogenolysis to yield 1,3-butadiene directly [196]. However, Kraus and Zdrazil argued that thiophene's chemistry indicates that the aromatic ring is hydrogenated to tetrahydrothiophene, which should be considered an intermediate [197]. This compound is typically reported in high-pressure thiophene HDS studies [198]. Additionally, partially hydrogenated thiophenes, such as 2,3-dihydrothiophene (2,3-DHT) and 2,5-dihydrothiophene (2,5-DHT), have been suggested as intermediates, although they were not detected in the gas phase [199]. Markel *et al*. determined that dihydrothiophenes are significantly more reactive than tetrahydrothiophene, which is, in turn, more reactive than thiophene [200].

Another unresolved issue is the origin of the periodic trends in HDS activity for various TMS. Beyond the industrially significant Co- or Ni-promoted MoS_2 and WS_2 catalysts, many TMS exhibit high hydrodesulfurization activity. Generally, Balandin volcano-type activity curves for these sulfides show maxima in thiophene HDS for the sulfides of Ir, Rh, and Co [201-203]. Harris and Chianelli interpreted this trend using the Sabatier principle [204], while Nørskov *et al*. suggested that activity is related to the TMS's ability to generate sulfur vacancies [205]. TMS with the lowest metal-sulfur bond energy will have the most sulfur vacancies and, consequently, the highest activity. Wiegand and Friend proposed that the most active materials are those that effectively activate the carbon-sulfur bond, implying that strong interactions between thiophene and TMS result in high activity [206]. Recent theoretical studies have shown that interactions between thiophene's sulfur atom and various TMS correlate well with HDS activity trends across the periodic table [207].

Intensive research aimed at understanding the nature of the active phase and the role of Co- or Ni-promoters has produced differing views on the synergistic effect in sulfided Co(Ni)Mo(W) catalysts. The 'Co-Mo-S' model [208, 209], the remote control model [210], and the rim-edge model [211] are among the most frequently used descriptions for the active phase in these catalysts. De Beer *et al*. proposed that MoS_2 primarily acts as a stabilizing carrier for highly dispersed Co- or Ni-sulfide particles [212, 213]. This view is supported by combined extended X-ray absorption fine structure (EXAFS) and Mössbauer Emission Spectroscopy measurements, indicating that small CoS_x ensembles are present at the MoS_2 crystallite edges and exhibit high HDS activity [214,215]. This finding aligns with the high thiophene HDS activity observed for metal sulfide clusters dispersed on a carbon support or occluded in zeolite micro-pores [216].

Operando and In-Situ Techniques

In situ techniques reveal new catalytic surface structures, compositions, and chemistry under working conditions, differing from vacuum measurements. This detailed information is crucial for catalyst design, offering insights into structure, bonding, and reactivity. These methods provide dynamic data under real reaction conditions, aiding theoretical calculations and optimizing catalyst efficiency. Thus, studying catalysts in their operative state with in situ/operando techniques is fundamental to catalysis research, greatly enhancing our understanding and control of catalytic processes [217].

In Situ Electron Microscopy for Catalysis Research

In Situ scanning and transmission electron microscopy (TEM)

In situ scanning [218] and transmission electron [219] microscopy have become crucial in catalysis research, providing subatomic spatial resolution and simultaneous atomic-level spectroscopy. This technology enables the analysis of critical interfaces and surfaces of individual catalysts, supported by various spectroscopy techniques. Over time, numerous in situ electron microscopy methods have been developed, each with distinct advantages highlighted in various review articles [220, 221].

In this review, we focus on electron microscopy techniques associated with cutting-edge advancements such as Four-Dimensional Scanning Transmission Electron Microscopy (4D-STEM) and those integrated with in situ synchrotron radiation techniques. The resolution of in situ TEM images depicting electrochemical processes in a liquid cell has been somewhat limited so far [222], partly due to challenges like high signal-to-noise ratios, enhanced spatial and temporal resolution, controlled environments, and a significant reduction in electron beam effects. Operando 4D-STEM diffraction imaging in liquid provides superior structural insights compared to traditional TEM/STEM imaging, thanks to its increased sensitivity and dynamic range [223].

Using a newly developed electron microscope pixel array detector (EMPAD), 4D-STEM can rapidly collect 2D electron diffraction patterns over a grid of probe positions, significantly reducing the electron dose while simultaneously gathering

nanoscale crystallographic data. This capability is essential for studying beam-sensitive materials in a liquid environment for catalysis. For instance, Yang *et al*. unveiled the structural complexity of active Cu sites using correlated electron and X-ray probes based on four-dimensional electrochemical liquid-cell scanning transmission electron microscopy, showcasing the power of advanced operando techniques for elucidating active sites in nanocatalysts [224].

In situ high-speed scanning tunneling microscopy (STM)

In situ high-speed scanning tunneling microscopy (STM) enables real-time atomic imaging [31], achieving a lateral resolution of approximately 100 pm and a vertical resolution of 1–3 pm at room temperature [66]. STM can observe individual atoms and their arrangements on a catalyst surface, offering unprecedented insights into catalytic mechanisms. For instance, Patera *et al*. demonstrated the catalytic role of single metal adatoms in the process of graphene growth on Ni using in situ STM [67]. Their research indicated that at high temperatures, carbon diffuses onto the nickel surface, promoting the growth of graphene islands with zigzag and Klein terminations. By monitoring layer formation at the atomic scale with millisecond time resolution through STM, the researchers observed mobile nickel adatoms at the kink sites of the graphene edges, acting as single-atom catalysts. Density functional theory calculations revealed that these adatoms strongly bind to the kinks, lower the energy barrier for carbon attachment, and facilitate the addition of carbon dimers, thus promoting graphene growth. This study provides atomic-level insights into graphene growth mechanisms, highlighting the potential of dynamic high-speed STM imaging for understanding surface processes at the atomic scale.

Additionally, high or ambient pressure combined with ambient temperature allows weakly interacting species to densely cover surfaces at room temperature in equilibrium with high gas pressure. This helps overcome activation barriers and trigger atomic structure reconstructions, often forming new structures for surface catalysts, as highlighted by high-pressure STM [66]. Overall, STM and transmission electron microscopy (TEM) are crucial for understanding catalysis at molecular and atomic levels in catalytic science. In situ STM excels at examining surface properties of single crystals, revealing detailed electronic and geometric aspects of catalysis. Conversely, in situ TEM is ideal for observing nanoparticle catalysts in real-time, shedding light on their structural changes and chemical reactions during the catalytic process [70].

These techniques provide complementary insights: TEM investigates how nanoparticle size affects catalysis, particularly at low-coordinated edge and corner sites, while STM examines the influence of atomic-scale structures on catalytic activity [71]. Additionally, they help study critical interactions within bimetallic nanoparticles, especially at metal-oxide interfaces, which are crucial for forming active catalytic sites [72–74]. Research in this field, supported by studies like those of Tsung *et al*. [70] and Somorjai *et al*. [71], underscores the roles of STM and TEM in revealing the intricate structural and chemical dynamics essential for catalysis. Together, they offer a comprehensive set of tools for catalysis research, enhancing our understanding of catalytic mechanisms and aiding in the development of more efficient, robust catalysts.

In Situ Synchrotron Radiation Techniques in Catalysis Research

Synchrotron radiation light sources, with their broad spectrum, high brightness, and coherence, have advanced beyond conventional methods in various applications, making significant contributions to catalysis research. These contributions include crystal and electronic structure analysis, surface composition assessments, and the detection of chemisorbed species and reactive intermediates [75]. A widely used technique is synchrotron radiation X-ray diffraction (SRXRD), which identifies crystalline materials and analyzes their structures [76]. By bombarding a sample with X-rays and examining the diffraction pattern, researchers can determine the atomic arrangement within the crystal structure. Scanning transmission X-ray microscopy (STXM) is an advanced microscopy technique that uses X-rays to produce high-resolution images of specimens. This method provides detailed information about the chemical state of a material at the nano-level, offering spatially resolved insights into the electronic and chemical structure of catalyst materials. STXM operates through a process called raster scanning, where an X-ray probe systematically moves across the specimen, capturing the intensity of transmitted X-rays at each position. By adding sample rotation, STXM can also perform tomography, yielding three-dimensional imaging of the specimen. The resolution in STXM depends on several factors, mainly the size of the X-ray spot, which is influenced by the coherence of the X-ray source, the precision of the experimental setup, and the performance of the focusing lenses. These factors collectively set the resolution limits of

STXM, similar to those observed in transmission X-ray nano-computed tomography [78].

Related studies on in situ STXM, including comparisons between STXM-XAS and STEM-EELS (scanning transmission electron microscopy–electron energy loss spectroscopy), have been summarized by Weckhuysen *et al.* [79], though they are not included here. Given the complex nature of catalytic reactions, developing synchrotron-radiation-based multi-techniques is essential for accurately capturing the dynamics of catalytic processes.

X-ray Absorption Spectroscopy (XAS)

X-ray absorption spectroscopy (XAS), encompassing XANES (X-ray absorption near-edge structure) and EXAFS, is widely employed for characterizing catalysts at the atomic level. XANES reveals the oxidation state and local symmetry of specific atoms, while EXAFS provides details about the local atomic structure [80]. XAS is instrumental in elucidating the local structure and chemical state of catalysts, offering insights into changes in their oxidation states during reactions [81, 82].

The NEXAFS (near-edge X-ray absorption fine structure) region of the spectrum pertains to excitations just above the ionization threshold, providing information about unfilled orbitals such as antibonding orbitals or unoccupied states in the solid-state density of states plot. This area yields insights into the chemical environment, including oxidation state, symmetry, and local charge distribution. In contrast, the EXAFS region arises from photoelectrons emitted from the atom and subjected to backscattering from neighboring electron clouds, yielding oscillations in X-ray energy that reveal details about the local environment, such as coordination numbers and distances to neighboring atoms.

In situ or operando XAS offers a significant advantage over conventional XAS by enabling real-time studies of chemical reactions under realistic operating conditions. Conducting in situ soft X-ray absorption spectroscopy (s-XAS) presents challenges, particularly in liquid-phase conditions, but offers unique advantages over hard X-ray (h-XAS) methods, especially in studying carbon, nitrogen, and oxygen-containing systems and surface-level interactions critical for catalyst studies [82]. Experimental challenges in s-XAS can be overcome using photon-in–photon-out techniques with a penetration depth of a few hundred nanometers, as demonstrated in studies like that of Sargent *et al.*, which employed density functional theory (DFT) calculations and in situ s-XAS to investigate multi-metal oxides for electrocatalytic applications [33].

Synchrotron radiation ambient pressure photoelectron spectroscopy (APPES)

Ambient-pressure photoelectron spectroscopy (APPES), particularly ambient-pressure X-ray photoelectron spectroscopy (APXPS) and ambient-pressure X-ray absorption spectroscopy (APXAS), provides insights into the electronic structure of catalysts, including their elemental composition, chemical state, and electronic states of the elements present [58, 89]. APXPS is especially useful for studying catalyst surfaces due to its shallow information depth, typically penetrating only a few nanometers (5–10 nm). For instance, Liu *et al.* investigated the interaction of oxygen gas with Cu (100) and Cu (111) single crystal surfaces using APXPS [90]. The combination of APXAS and APXPS offers complementary information about a material: APXPS provides detailed surface chemistry and electronic structure insights, while APXAS reveals properties deeper within the material. In contrast, ambient-pressure mapping of resonant Auger electron spectroscopy (AP-mRAS) enhances XAS data collection by employing Auger electron yield (AEY) mode with kinetic energy resolution. This approach, compared to traditional XAS, adds a dimension along the kinetic energy of emitted Auger electrons at each resonant energy. Thus, AP-mRAS can elucidate valence and unoccupied states near the absorption edge with greater sensitivity to electronic states. Moreover, AP-mRAS captures details of secondary decay processes at different photon energies, distinguishing non-resonant or normal Auger and resonant Auger processes.

Infrared (IR) spectroscopy

Infrared spectroscopy combined with scanning probe microscopy enables precise analysis of heterogeneous materials at the nanoscale. Synchrotron infrared nano-spectroscopy enhances this capability by employing low-noise, broadband synchrotron infrared radiation, enabling comprehensive spatio-spectral analysis for catalysis research [93]. The catalytic performance of heterogeneous catalysts correlates closely with the coordination number of surface atoms. Surface defects and edge regions often exhibit enhanced catalytic activity due to their lower-coordinated surface atoms. Directly assessing the catalytic activity at different sites on metal nanoparticles is essential for understanding heterogeneous catalysis mechanisms. However,

conventional infrared and Raman spectroscopies are limited in spatial resolution and cannot achieve this goal. High-spatial-resolution synchrotron-radiation-based infrared nano-spectroscopy (SINS) addresses this gap by mapping site-specific differences in reactivity on single particles. Infrared nano-spectroscopy line scans conducted after exposing the sample to various reaction conditions can directly probe differences in catalytic activity between sites on metal nanoparticles.

Interpreting the large and complex datasets generated often requires advanced computational methodologies and significant domain expertise. Furthermore, experimental conditions achievable at synchrotron facilities may not fully replicate industrial process conditions, posing potential limitations in directly translating research findings. Therefore, while synchrotron radiation techniques are indispensable, their application requires careful consideration of these inherent constraints.

In situ solid‑state Nuclear Magnetic Resonance (NMR) Techniques for Catalysis Research

In situ solid-state NMR has emerged as a powerful tool for investigating catalytic mechanisms. This technique allows for real-time monitoring of catalytic reactions, enabling the identification of reaction intermediates, study of structural changes in catalysts and reactants, and exploration of host-guest interactions with catalysts under conditions closely mimicking real reaction environments at the molecular level. Currently, two main types of in-situ solid-state NMR technologies are prominent: batch-like setups [95] and continuous-flow systems [96]. In batch-like setups, the catalyst is prepared with reactants outside the NMR probe, loaded into the rotor, and then transferred to the probe for heating to the reaction temperature while acquiring NMR spectra throughout the process. This method is straightforward and widely applicable for catalytic reactions conducted under high temperature and pressure conditions.

However, most reactions occur under continuous flow conditions, which differ significantly from static methods. Variations in flow rate can lead to different reaction outcomes. Continuous-flow NMR technology addresses this by enabling investigations of reaction mechanisms under realistic flow conditions, particularly valuable for studying heterogeneous catalysis. This approach closely replicates actual catalytic reaction processes, facilitating breakthroughs in understanding reaction mechanisms, capturing reaction intermediate species, and elucidating reaction kinetics. For instance, Hunger *et al.* [100–102] utilized continuous-flow NMR to explore the methanol-to-olefin (MTO) mechanism, highlighting the significance of surface methoxy species as crucial intermediates in C–C bond formation.

In summary, this section underscores fundamental catalysis principles such as adsorption-desorption dynamics, surface reactions, and active site influences on catalytic outcomes. It emphasizes the pivotal roles of in situ TEM and STM in probing molecular-scale factors affecting catalytic behavior. Additionally, synchrotron radiation techniques have revolutionized catalysis research by offering unparalleled sensitivity and detail through innovations like storage rings, insertion devices, and high-energy lattices. To comprehensively understand catalytic properties at the molecular scale, integrating in situ and operando techniques is essential. Electron microscopy provides atomic-level spatial resolution, revealing dynamic catalyst structures under reaction conditions. Spectroscopic methods such as XAS (X-ray absorption spectroscopy), encompassing XANES and EXAFS, offer insights into electronic structures and coordination environments of catalytic sites crucial for understanding reactant activation and transformation. Synchrotron-based techniques enhance these spectroscopic capabilities with higher intensity and resolution, enabling the study of rapid and transient catalytic phenomena. By combining insights from these techniques, researchers can advance our understanding of catalysis, bridging studies from nanoparticles to single crystals to gain a comprehensive understanding of factors governing catalytic efficiency and selectivity. For example, high-resolution IR spectroscopy, coupled with scanning probe microscopy, provides detailed insights into the coordination numbers of surface atoms and their impact on catalytic activity.

Conclusions

ULSD fuels are being developed to diminish of sulfur concentrations for reaching to 10.0 ppm or less to restrain air pollution. Advanced HDS processes are required to achieve zero sulfur emissions, but developing new processes requires high investment. Therefore, improving the design of high-performance catalysts is a more viable solution, which has the potential to be customized to existing HDS process units. These various catalysts must eradicate intricate sulfur compounds through a pathway of direct HDS reactions, operate at medium pressure with low space velocity values, and exhibit exceptional stability.

Catalysts that have been promoted by transition metals have been promising for many years, but precise tuning is required for high-performance operation. The alumina support can be possible improved the metal-support interaction by introducing new additive species or by adding a secondary support that has complementary property of surface, which can improve active phase morphology and introduce better selectivity state with long-terms stabilities.

Several factors, including metal dispersion over supports, metals-supports interaction, active phase morphology, and stability of catalyst, are determining factors for the catalytic removal of sulfur from refractive compounds to achieve ultra low sulfur diesel. Additive species can alter the interactions between the metal and the support material and improve catalyst stability to acquire active phases of type-II, which are comparatively exhibiting a higher level of activity than type-I and has lower interaction with the support. The dispersion factor, which includes the morphology parameters such as the number of stacked layers and the measurement of the slabs, is also a crucial aspect to enhance for effectively eliminating sulfur from compounds such as DBT and its derivatives that display recalcitrance. The chelating agents using can improve metal dispersion and enhance the involvement of promoter atoms in phases that are not stoichiometric, while delaying sulfidation and suppressing bulk sulfide formation. Catalysts that are not supported and are obtained from transition sulfides containing multiple metals offer great opportunities to enhance the catalytic properties of HDS for increasingly rigorous the process conditions. Different morphologies and promoters to additives can be inserted to get better activity or property of selectivity. Modelation ways using the advance theoretically calculations can further predict the peculiarities of TMS catalyst via generating empirical HDS outcomes and the properties related to electricity of catalysts that are being tested in experiments.

Lastly, the development of new, better-performing catalysts for TMS is optimistic, with recent experimental and theoretical reports showing great potential for meeting societally needs in the near and far future.

References

1. J. N. Díaz de León, C. Ramesh Kumar, J. Antúnez-García and S. Fuentes-Moyado, Recent insights in transition metal sulfide hydrodesulfurization catalysts for the production of ultra-low sulfur diesel: A short review, *Catal.*, **9**, 87 (2019).
2. E. Wang, F. Yang, M. Song, G. Chen, Q. Zhang, F. Wang and D. Han, Recent advances in the unsupported catalysts for the hydrodesulfurization of fuel, *Fuel Process. Technol.*, **235**, 107386 (2022).
3. S. Mendiratta and A. Ali, Recent advances in functionalized mesoporous silica frameworks for efficient desulfurization of fuels, *Nanomaterials*, **10**, 6 (2020).
4. J. D. De León, L. A. Zavala-Sánchez, V. A. Suárez-Toriello, G. Alonso-Núñez, T. A. Zepeda, R. I. Yocupicio and S. Fuentes, Support effects of NiW catalysts for highly selective sulfur removal from light hydrocarbons, *Appl. Catal. B Environ.*, **213**, 167 (2017).
5. T. Zhang, J. Zhang, Z. Wang, J. Liu, G. Qian, D. Wang and X. Gong, Review of electrochemical oxidation desulfurization for fuels and minerals, *Fuel*, **305**, 121562 (2021).
6. S. Sánchez, R. Sánchez and E. Barleta, CO_2 emissions in Latin American maritime imports and revised export calculations, **212**, 160 (2021).
7. J. N. Díaz de León, C. Ramesh Kumar, J. Antúnez-García and S. Fuentes-Moyado, Recent insights in transition metal sulfide hydrodesulfurization catalysts for the production of ultra-low sulfur diesel: A short review, *Catal.*, **9**, 87 (2019).
8. S. Hansen, A. Mirkouei and L. A. Diaz, A comprehensive state-of-technology review for upgrading bio-oil to renewable or blended hydrocarbon fuels, *Renew. Sustain. Energy Rev.*, **118**, 109548 (2020).
9. R. Saab, K. Polychronopoulou, L. Zheng, S. Kumar and A. Schiffer, Synthesis and performance evaluation of hydrocracking catalysts: A review, *J. Ind. Eng. Chem.*, **89**, 83 (2020).
10. A. Tanimu, , & K. Alhooshani, Advanced hydrodesulfurization catalysts: a review of design and synthesis, *Energy & Fuels*, **33**(4), 2810–2838 (2019).
11. M. D. Mello, F. A. Braggio, B. C. Magalhães, J. L. Zotin and M. A. P. Silva, Kinetic modeling of deep hydrodesulfurization of dibenzothiophenes on NiMo/alumina catalysts modified by phosphorus, *Fuel Process. Technol.*, **177**, 66 (2018).
12. N. Salazar, S. B. Schmidt and J. V. Lauritsen, Adsorption of nitrogenous inhibitor molecules on MoS_2 and CoMoS hydrodesulfurization catalyst particles investigated by scanning tunneling microscopy, *J. Catal.*, **370**, 232 (2019).
13. M. Mallet, I. Naboulsi, B. Lebeau, C. F. L. Aponte, S. Brunet, L. Michelin, M. Bonne, C. Carteret and J. L. Blin, Selective direct desulfurization way (DDS) with CoMoS supported over mesostructured titania for the deep hydrodesulfurization of 4,6-dimethyldibenzothiophene, *Appl. Catal. A Gen.*, **563**, 91 (2018).

14. M. F. Wagenhofer, Unsupported transition metal sulfides for hydrotreating of conventional and renewable feedstock, Ph.D. Thesis, Technische Universität München, (2020).
15. J. Kaur, Oxidative desulfurization of tire pyrolysis oil over molybdenum heteropolyacid supported mesoporous catalysts, Ph.D. Thesis, University of Saskatchewan, (2022).
16. H. Nie, H. Li, Q. Yang and D. Li, Effect of structure and stability of active phase on catalytic performance of hydrotreating catalysts, *Catal. Today*, **316**, 13–20 (2018).
17. M. H. Ibrahim, M. Hayyan, M. A. Hashim and A. Hayyan, The role of ionic liquids in desulfurization of fuels: A review, *Renew. Sustain. Energy Rev.*, **1534–1549** (2017).
18. R. Gatan, P. Barger, V. Gembicki, A. Cavanna and D. Molinari, Oxidative desulfurization: A new technology for ULSD, *Am. Chem. Soc. Div. Fuel Chem.*, **49**, 577–579 (2004).
19. A. G. Olaremu and W. R. Adedoyin, Hydrodesulphurization of Bonny light crude oil using nano Co–Mo supported on zeolite synthesized from Akoko clay, *Mater. Rep. Energy*, **2.4**, 100162 (2022).
20. E. Wang, F. Yang, M. Song, G. Chen, Q. Zhang, F. Wang, ... and D. Han, Recent advances in the unsupported catalysts for the hydrodesulfurization of fuel, *Fuel Process. Technol.*, **235**, 107386 (2022).
21. A. M. Venezia, V. L. Parola and L. F. Liotta, "Structural and surface properties of heterogeneous catalysts: Nature of the oxide carrier and supported particle size effects", *Catal. Today*, **285**, 114–124 (2017).
22. Y. Gutiérrez, S. Singh, E. Schachtl, J. Kim, E. Kondratieva, J. Hein and J. A. Lercher, "Effects of the Support on the Performance and Promotion of (Ni)MoS_2 Catalysts for Simultaneous Hydrodenitrogenation and Hydrodesulfurization", *ACS Catal.*, **4**, 1487–1499 (2014).
23. Z. S. Mahmoudabadi, A. Rashidi and M. Panahi, New approach to unsupported ReS_2 nanorod catalyst for upgrading of heavy crude oil using methane as hydrogen source, *Int. J. Hydrogen Energy*, **46**, 5270–5285 (2021).
24. H. Topsoe, The role of Co–Mo–S type structures in hydrotreating catalysts, *Appl. Catal. A Gen.*, **322**, 3–8 (2007).
25. Okamoto, Y., Maezawa, A., & Imanaka, T., Active sites of molybdenum sulfide catalysts supported on Al_2O_3 and TiO_2 for hydrodesulfurization and hydrogenation, *J. Catal.*, **120**, 29-45 (1989).
26. A. Haruna, Z. M. A. Merican, S. G. Musa and S. Abubakar, Sulfur removal technologies from fuel oil for safe and sustainable environment, *Fuel*, **329**, 125370 (2022).
27. C. Bara, A. F. Lamic-Humblot, E. Fonda, A. S. Gay, A. E. Taleb, E. Devers, M. Digne, G. D. Pirngruber and X. Carrier, Surface-Dependent Sulfidation and Orientation of MoS_2 Slabs on Alumina-Supported Model Hydrodesulfurization Catalysts, *J. Catal.*, **344**, 591–605 (2016).
28. Y. Sakashita, Y. Araki, K. Honna, H. Shimada, Orientation and Morphology of Molybdenum Sulfide Catalysts Supported on Titania Particles, Observed by Using High-Resolution Electron Microscopy, *Appl. Catal. A Gen.*, **197**, 247–253 (2000).
29. C. Arrouvel, M. Breysse, H. Toulhoat, P. Raybaud, A Density Functional Theory Comparison of Anatase (TiO_2)- and γ-Al_2O_3-Supported MoS_2 Catalysts, *J. Catal.*, **232**, 161–178 (2005).
30. G. Berhault, *New Materials for Catalytic Applications*, Elsevier, Amsterdam, The Netherlands, Vol. 10, p. 336 (2016).
31. A. Nogueira, R. Znaiguia, D. Uzio, P. Afanasiev and G. Barhault, Curved Nanostructures of Unsupported and Al_2O_3-Supported MoS_2 Catalysts: Synthesis and HDS Catalytic Properties, *Appl. Catal. A Gen.*, **429–430**, 92–105 (2012).
32. J. N. Díaz de León, J. A. García, G. A. Nuñez, T. A. Zepeda, D. H. Galvan, J. A. de los Reyes and S. Fuentes-Moyado, Support Effects of NiW Hydrodesulfurization Catalysts from Experiments and DFT Calculations, *Appl. Catal. B Environ.*, **238**, 480–490 (2018).
33. Y. Iwata, Y. Araki, K. Honna, Y. Miki, K. Sato and H. Shimada, Hydrogenation Active Sites of Unsupported Molybdenum Sulfide Catalysts for Hydroprocessing Heavy Oils, *Catal. Today*, **65**, 335–341 (2001).
34. P. Afanasiev, Topotactic Synthesis of Size-Tuned MoS_2 Inorganic Fullerenes That Allows Revealing Particular Catalytic Properties of Curved Basal Planes, *Appl. Catal. B Environ.*, **227**, 44–53 (2018).
35. R.O. Estrella, J.L.G. Fierro, J.N. Díaz de León, S. Fuentes, G.A. Nuñez, E.L. Medina, B. Pawelec, T.A. Zepeda, Effect of Partial Mo Substitution by W on HDS Activity Using Sulfide CoMoW/Al_2O_3–TiO_2 Catalysts, *Fuel*, **233**, 644–657 (2018).
36. A. García-Vila, R. Cuevas-García, J. Ramírez, I. Puente-Lee, Effect of Phosphorus on Mo/Al_2O_3 Catalysts for Maya Crude Improvement, *Catal. Today*, **220-222**, 310–317 (2014).
37. D. Laurenti, B.P. Ngoc, L. Massin, C. Roukoss, E. Devers, K. Marchand, L. Lemaitre, C. Legens, A.A. Quoineaud, M. Vrinat, Intrinsic Potential of Alumina-Supported CoMo Catalysts in HDS: Comparison Between γc, γT, and δ-Alumina, *J. Catal.*, **297**, 165–175 (2013).
38. Y. Araki, K. Honna, H. Shimada, Formation and Catalytic Properties of Edge-Bonded Molybdenum

Sulfide Catalysts on TiO_2, *J. Catal.*, **207**, 361–370 (2002).
39. H. Wang, C. Wang, B. Xiao, L. Zhao, J. Zhang, Y. Zhu, X. Guo, The hydroxyapatite nanotube as promoter to optimize the HDS reaction of $NiMo/TiO_2$ catalysts, *Catal. Today*, **259**, 340–346 (2016).
40. P. Platanitis, G.D. Panagiotou, K. Bourikas, C. Kordulis, J.L.G. Fierro, A. Lycourghiotis, Preparation of un-promoted molybdenum HDS catalysts supported on titania by equilibrium deposition filtration: Optimization of the preparative parameters and investigation of the promoting action of titania, *J. Mol. Catal. A Chem.*, **412**, 1–12 (2016).
41. P.C. Villalón, J. Ramírez, R. Cuevas, P. Vázquez, Influence of the support on the catalytic performance of Mo, CoMo, and NiMo catalysts on Al_2O_3 and TiO_2 during the HDS of thiophene, dibenzothiophene, or 4,6-dimethyldibenzothiophene, *Catal. Today*, **259**, 140–149 (2016).
42. A. Haruna, Z. M. A. Merican, S. G. Musa, & S. Abubakar, Sulfur removal technologies from fuel oil for safe and sustainable environment, *Fuel*, **329**, 125370 (2022).
43. D. Laurenti, T. K. T. Ninh, N. Escalona, L. Massin, M. Vrinat, F. J. G. Llambías, Support effect with rhenium sulfide catalysts, *Catal. Today*, **130**, 50–55 (2008).
44. T. K. Ninh, D. Laurenti, E. Leclerc, M. Vrinat, Support effect for CoMoS and CoNiMoS hydrodesulfurization catalysts prepared by controlled method, *Appl. Catal. A Gen.*, **487**, 210–218 (2014).
45. S. Badoga, R. V. Sharma, A. K. Dalai, J. Adjaye, Hydrotreating of heavy gas oil on mesoporous zirconia supported NiMo catalyst with EDTA, *Fuel*, **128**, 30–38 (2014).
46. F. K. Mahdi, M. T. Albdiry, A. A. Diwan, Preparation and Catalytic Activity of Co-Mo/γ-Al_2O_3 Catalyst for Hydro-desulfurization Reaction, (2020).
47. S. Song, X. Zhou, A. Duan, Z. Zhao, K. Chi, M. Zhang, G. Jiang, J. Liu, J. Li, X. Wang, Synthesis of mesoporous silica material with ultra-large pore sizes and the HDS performance of dibenzothiophene, *Microporous Mesoporous Mater.*, **226**, 510–521 (2016).
48. H. Y. Zhu, N. Y. Shi, D. Y. Liu, R. Li, J. G. Yu, Q. T. Ma, ... & W. Y. Guo, New insights into the mechanism of reactive adsorption desulfurization on Ni/ZnO catalysts: Theoretical evidence showing the existence of interfacial sulfur transfer pathway and the essential role of hydrogen, *Petroleum Science*, **20(5)**, 3240-3250 (2023).
49. N. Al-zaqri, A. Alsalme, S.F. Adil, A. Alsaleh, S.G. Alshammari, S.I. Alresayes, R. Alotaibi, M. Al-Kinany, M.R.H. Siddiqui, Comparative catalytic evaluation of nickel and cobalt substituted phosphomolybdic acid catalyst supported on silica for hydrodesulfurization of thiophene, *J. Saudi Chem. Soc.*, **21**, 965–973 (2017).
50. J.N. Díaz de León, Binary γ-Al_2O_3–α-Ga_2O_3 as supports of NiW catalysts for hydrocarbon sulfur removal, *Appl. Catal. B Environ.*, **181**, 524–533 (2016).
51. R.O. Estrella, J.L. Fierro, J.N. Díaz de León, S. Fuentes, G.A. Nuñez, E.L. Medina, B. Pawelec, T.A. Zepeda, Effect of partial Mo substitution by W on HDS activity using sulfide $CoMoW/Al_2O_3$–TiO_2 catalysts, *Fuel*, **233**, 644–657 (2018).
52. G. Wan, A. Duan, Z. Zhao, D. Zhang, R. Li, T. Dou, Al_2O_3−TiO_2/Al_2O_3−TiO_2−SiO_2 Composite-Supported Bimetallic Pt−Pd Catalysts for the Hydrodearomatization and Hydrodesulfurization of Diesel Fuel, *Energy Fuels*, **23**, 81–85 (2009).
53. T. O., Dembaremba, T., Majodina, R. S., Walmsley, A. S., Ogunlaja, & Z. R Tshentu, Perspectives on strategies for improving ultra-deep desulfurization of liquid fuels through hydrotreatment: Catalyst improvement and feedstock pre-treatment, *Front. Chem.*, **10**, 807225 (2022).
54. J. A., Tavizon-Pozos, V. A., Suarez-Toriello, J. A., de los Reyes, A. G., Lara, M., Fierro, & C., Geantet, Deep Hydrodesulfurization of Dibenzothiophenes over NiW Sulfide Catalysts Supported on Sol–Gel Titania–Alumina, *Top. Catal.*, **59**, 241–251 (2016).
55. H. Wang, Z. Yao, X. Zhan, Y. Wu, and M. Li, Preparation of Highly Dispersed W/ZrO_2–Al_2O_3 Hydrodesulfurization Catalysts at High WO_3 Loading via a Microwave Hydrothermal Method, *Fuel*, **158**, 918–926 (2015).
56. I. Vazquez-Garrido, A.L. Benítez, G. Berhault, and A. Guevara-Lara, Effect of Support on the Acidity of $NiMo/Al_2O_3$-MgO and $NiMo/TiO_2$-Al_2O_3 Catalysts and on the Resulting Competitive Hydrodesulfurization/Hydrodenitrogenation Reactions, *Fuel*, **236**, 55–64 (2019).
57. M. Saeed, et al., MOFs for Desulfurization of Fuel Oil: Recent Advances and Future Insights, *J. Chin. Chem. Soc.*, 70, 789–824 (2023).
58. J. Escobar, J.A. De Los Reyes, C.A. Ulín, M.C. Barrera, Highly Active Sulfided CoMo Catalysts Supported on $(ZrO_2$–$TiO_2)/Al_2O_3$ Ternary Oxides, *Mater. Chem. Phys.*, **143**, 213–222 (2013).
59. P. Jabbarnezhad, M. Haghighi, P. Taghavinezhad, Sonochemical Synthesis of $NiMo/Al_2O_3$–ZrO_2 Nanocatalyst: Effect of Sonication and Zirconia Loading on Catalytic Properties and Performance in Hydrodesulfurization Reaction, *Fuel Process. Technol.*, **126**, 392–401 (2014).

60. M.A. Daous, S.A. Ali, Deep Desulfurization of Gas Oil over NiMo Catalysts Supported on Alumina–Zirconia Composites, *Fuel*, **97**, 662–669 (2012).
61. E. Prado-Baston, A. Boscaro-Franca, A.V. da Silva Neto, E.A. Urquieta-Gonzalez, Incorporation of the Precursors of Mo and Ni Oxides Directly into the Reaction Mixture of Sol–Gel Prepared γ-Al_2O_3-ZrO_2 Supports – Evaluation of the Sulfided Catalysts in the Thiophene Hydrodesulfurization, *Catal. Today*, **246**, 184–190 (2015).
62. A.E. Cruz-Pérez, Y.T. Jiménez, J. V. Alejo, T.A. Zepeda, D.M. Márquez, G.R. Ruedas, S. Fuentes-Moyado, J.N. Díaz de León, NiW/MgO–TiO_2 Catalysts for Dibenzothiophene Hydrodesulfurization: Effect of Preparation Method, *Catal. Today*, **271**, 28–34 (2016).
63. J.C. Betancourt, A.L. Benítez, J.R. López, L. Massin, M. Aouine, M. Vrinat, G. Berhault, A.G. Lara, Interaction Effects of Nickel Polyoxotungstate with the Al_2O_3–MgO Support for Application in Dibenzothiophene Hydrodesulfurization, *J. Catal.*, **313**, 9–23 (2014).
64. A.L. Benitez, G. Berhault, A.G. Lara, Addition of Manganese to Alumina and Its Influence on the Formation of Supported NiMo Catalysts for Dibenzothiophene Hydrodesulfurization Application, *J. Catal.*, **344**, 59–76 (2016).
65. A.L. Benitez, G. Berhault, L. Burel, A.G. Lara, Novel NiW Hydrodesulfurization Catalysts Supported on Sol-Gel Mn-Al_2O_3, *J. Catal.*, **354**, 197–212 (2017).
66. A.L. Benitez, G. Berhault, A.G. Lara, NiMo Catalysts Supported on Mn-Al_2O_3 for Dibenzothiophene Hydrodesulfurization Application, *Appl. Catal. B Environ.*, **213**, 28–41 (2017).
67. F. Trejo, M.M. Rana, J. Ancheyta, S. Chavez, Influence of Support and Supported Phases on Catalytic Functionalities of Hydrotreating Catalysts, *Fuel*, **138**, 104–110 (2014).
68. A. Nishijima, H. Shimada, T. Sato, Y. Yoshimura, J. Hiraishi, Support Effects on Hydrocracking and Hydrogenation Activities of Molybdenum Catalysts Used for Upgrading Coal-Derived Liquids, *J. Polyhedron*, **5**, 243–247 (1986).
69. J. Ramirez, P. Rayo, A.G. Alejandre, J. Ancheyta, M.S. Rana, Analysis of the Hydrotreatment of Maya Heavy Crude with NiMo Catalysts Supported on TiO_2-Al_2O_3 Binary Oxides: Effect of the Incorporation Method of Ti, *Catal. Today*, **109**, 54–60 (2005).
70. N. Coville, T.O. Dembaremba, S. Majodina, R.S. Walmsley, A.S. Ogunlaja, Z.R. Tshentu, 15 Years of the Federation of African Societies of Chemistry (FASC), (2022).
71. S. Sheibani, K. Zare, S.M. Mousavi Safavi, The Effects of pH and Chelating Agent on Synthesis and Characterization of NiMo/γ-Alumina Nanocatalyst for Heavy Oil Hydrodesulfurization, *Iranian J. Chem. Chem. Eng.*, **40**(1), 21–34 (2021).
72. Y. Zhu, Q.M. Ramasse, M. Brorson, P.G. Moses, L.P. Hansen, C.F. Kisielowski, S. Helveg, Visualizing the Stoichiometry of Industrial-Style Co-Mo-S Catalysts with Single-Atom Sensitivity, *Angew. Chem. Int. Ed.*, **53**, 10723–10727 (2014).
73. V.A. Suarez-Toriello, C.E.S. Vargas, J.A. de los Reyes, A.V. Zavala, M. Vrinat, C. Geantet, Influence of the Solution pH in Impregnation with Citric Acid and Activity of Ni/W/Al_2O_3 Catalysts, *J. Mol. Catal. A Chem.*, **404–405**, 36–46 (2015).
74. I.E. Wachs, K. Routray, Catalysis Science of Bulk Mixed Oxides, *ACS Catal.*, **2**(6), 1235–1246 (2012).
75. Z. S. Mahmoudabadi, A. Tavasoli, A. Rashidi, and M. Esrafili, Catalytic Activity of Synthesized 2D MoS_2/Graphene Nanohybrids for the Hydrodesulfurization of SRLGO: Experimental and DFT Study, *Environ. Sci. Pollut. Res.*, **28**, 5978–5990 (2021).
76. E.J. Hensen, Y.V. der Meer, J.A. Veen, J.W. Niemantsverdriet, Insight into the Formation of the Active Phases in Supported NiW Hydrotreating Catalysts, *Appl. Catal. A Gen.*, **322**, 16–32 (2007).
77. L. Coulier, V.H. de Beer, J.A. van Veen, J.W. Niemantsverdriet, Correlation between Hydrodesulfurization Activity and Order of Ni and Mo Sulfidation in Planar Silica-Supported NiMo Catalysts: The Influence of Chelating Agents, *J. Catal.*, **197**, 26–33 (2001).
78. Y. Okamoto, A. Kato, S. Usman, K. Sato, T. Kubota, Co–WS_2 Hydrodesulfurization Catalysts: An Unexpected More Favorable Combination than Co–MoS_2, *Chem. Lett.*, **34**, 1258–1259 (2005).
79. T. Kubota, N. Miyamoto, M. Yoshioka, Y. Okamoto, Surface Structure and Sulfidation Behavior of Co-Mo and Co-W Sulfide Catalysts for the Hydrodesulfurization of Dibenzothiophene, *Appl. Catal. A Gen.*, **480**, 10–16 (2014).
80. A.C. Pierre, A.C. Pierre, Applications of Sol-Gel Processing, *Introduction to Sol-Gel Processing*, 597–685 (2020).
81. G. Kishan, L. Coulier, J.A.R. van Veen, J.W. Niemantsverdriet, Promoting Synergy in CoW Sulfide Hydrotreating Catalysts by Chelating Agents, *J. Catal.*, **200**, 194–196 (2001).
82. J. Escobar, M.C. Barrera, A.W. Gutierrez, M.A.C. Jacome, C.A. Chavez, J.A. Toledo, D.A.S. Casados, Highly Active P-Doped Sulfided NiMo/Alumina HDS Catalysts from Mo-Blue by Using Saccharose as Reducing Agents Precursor, *Appl. Catal. B Environ.*, **237**, 708–720 (2018).
83. P. Mazoyer, C. Geantet, F. Diehl, S. Loridant, M. Lacroix, Role of Chelating Agent on the Oxidic State of Hydrotreating Catalysts, *Catal. Today*, **130**, 75–79 (2008).

84. A.M. de Jong, V.H.J. de Beer, J.A.R. van Veen, J.W. Niemantsverdriet, Surface Science Model of a Working Cobalt-Promoted Molybdenum Sulfide Hydrodesulfurization Catalyst: Characterization and Reactivity, *J. Phys. Chem.*, **100**, 17722–17724 (1996).
85. L. Medici, R. Prins, The Influence of Chelating Ligands on the Sulfidation of Ni and Mo in $NiMo/SiO_2$ Hydrotreating Catalysts, *J. Catal.*, **163**, 38–49 (1996).
86. L. Van Haandel, G.M. Bremmer, E.J.M. Hensen, T. Weber, The Effect of Organic Additives and Phosphoric Acid on Sulfidation and Activity of $(Co)Mo/Al_2O_3$ Hydrodesulfurization Catalysts, *J. Catal.*, **351**, 95–106 (2017).
87. P. Blanchard, C. Lamonier, A. Griboval, E. Payen, New Insight in the Preparation of Alumina Supported Hydrotreatment Oxidic Precursors: A Molecular Approach, *Appl. Catal. A Gen.*, **322**, 33–45 (2007).
88. A.V. Pashigreva, G.A. Bukhtiyarova, O.V. Klimov, Y.A. Chesalov, G.S. Litvak, A.S. Noskov, Activity and Sulfidation Behavior of the $CoMo/Al_2O_3$ Hydrotreating Catalyst: The Effect of Drying Conditions, *Catal. Today*, **149**, 19–27 (2010).
89. B. Wang, W. Yu, D. Meng, Z. Li, Y. Xu, X. Ma, Effect of Citric Acid on $CoO–MoO_3/Al_2O_3$ Catalysts for Sulfur-Resistant Methanation, *React. Kinet. Mech. Catal.*, **125**, 111–126 (2018).
90. M. Taghizadeh, E. Mehrvarz, A. Taghipour, Polyoxometalate as an Effective Catalyst for the Oxidative Desulfurization of Liquid Fuels: A Critical Review, *Rev. Chem. Eng.*, **36**, 831–858 (2020).
91. M.A. Magdaleno, J.A. Nieto, T.E. Klimova, Effect of the Amount of Citric Acid Used in the Preparation of NiMo/SBA-15 Catalysts on Their Performance in HDS of Dibenzothiophene-Type Compounds, *Catal. Today*, **220–222**, 78–88 (2014).
92. H. Wu, A. Duan, Z. Zhao, D. Qi, J. Li, B. Liu, G. Jiang, J. Liu, Y. Wei, X. Zhang, Preparation of NiMo/KIT-6 Hydrodesulfurization Catalysts with Tunable Sulfidation and Dispersion Degrees of Active Phase by Addition of Citric Acid as Chelating Agent, *Fuel*, **130**, 203–210 (2014).
93. J. Chen, F. Maugé, J.E. Fallah, L. Oliviero, IR Spectroscopy Evidence of MoS_2 Morphology Change by Citric Acid Addition on MoS_2/Al_2O_3 Catalysts—A Step Forward to Differentiate the Reactivity of M-Edge and S-Edge, *J. Catal.*, **320**, 170–179 (2014).
94. P.A. Nikulshin, D.I. Ishutenko, A.A. Mozhaev, K.I. Maslakov, A.A. Pimerzin, Effects of Composition and Morphology of Active Phase of $CoMo/Al_2O_3$ Catalysts Prepared Using Co_2Mo10–Heteropolyacid and Chelating Agents on Their Catalytic Properties in HDS and HYD Reactions, *J. Catal.*, **312**, 152–169 (2014).
95. J. Chen, F. Maugé, J. El Fallah, and L. Oliviero, IR Spectroscopy Evidence of MoS_2 Morphology Change by Citric Acid Addition on MoS_2/Al_2O_3 Catalysts–A Step Forward to Differentiate the Reactivity of M-Edge and S-Edge, *J. Catal.*, **320**, 170–179 (2014).
96. H. Li, M. Li, Y. Chu, F. Liu, H. Nie, Essential Role of Citric Acid in Preparation of Efficient NiW/Al_2O_3 HDS Catalysts, *Appl. Catal. A Gen.*, **403**, 75–82 (2011).
97. Z. S. Mahmoudabadi, A. Rashidi, and M. Panahi, New Approach to Unsupported ReS_2 Nanorod Catalyst for Upgrading of Heavy Crude Oil Using Methane as Hydrogen Source, *Int. J. Hydrogen Energy*, **46**(7), 5270–5285 (2021).
98. D. Valencia, T. Klimova, Citric Acid Loading for MoS2-Based Catalysts Supported on SBA-15. New Catalytic Materials with High Hydrogenolysis Ability in Hydrodesulfurization, *Appl. Catal. B Environ.*, **129**, 137-145 (2013).
99. T.E. Klimova, D. Valencia, J.A. Nieto, P.H. Hipólito, Behavior of NiMo/SBA-15 Catalysts Prepared with Citric Acid in Simultaneous Hydrodesulfurization of Dibenzothiophene and 4,6-Dimethyldibenzothiophene, *J. Catal.*, **304**, 29-46 (2013).
100. P.C. Villalón, J. Ramirez, J.V. Luciano, Analysis of the Role of Citric Acid in the Preparation of Highly Active HDS Catalysts, *J. Catal.*, **320**, 127-136 (2014).
101. F. K. Mahdi, M. T. Albdiry, and A. A. Diwan, Preparation and Catalytic Activity of $Co-Mo/\gamma-Al_2O_3$ Catalyst for Hydro-desulfurization Reaction, (2020).
102. N.Q. Bui, C. Geantet, G. Berhault, Maleic Acid, an Efficient Additive for the Activation of Regenerated $CoMo/Al_2O_3$ Hydrotreating Catalysts, *J. Catal.*, **330**, 374-386 (2015).
103. A. Pimerzin, A. Roganov, A. Mozhaev, K. Maslakov, P. Nikulshin, A. Pimerzin, Active Phase Transformation in Industrial $CoMo/Al_2O_3$ Hydrotreating Catalyst During Its Deactivation and Rejuvenation with Organic Chemicals Treatment, *Fuel Process. Technol.*, **173**, 56-65 (2018).
104. Y. Zhang, W. Han, X. Long, H. Nie, Redispersion Effects of Citric Acid on $CoMo/\gamma-Al_2O_3$ Hydrodesulfurization Catalysts, *Catal. Commun.*, **82**, 20-23 (2016).
105. W. Han, H. Nie, X. Long, M. Li, Q. Yang, D. Li, Preparation of F-Doped MoS_2/Al_2O_3 Catalysts as a Way to Understand the Electronic Effects of the Support Brønsted Acidity on HDN Activity, *J. Catal.*, **339**, 135-142 (2016).
106. W. Han, H. Nie, X. Long, M. Li, Q. Yang, D. Li, Effects of the Support Brønsted Acidity on the Hydrodesulfurization and Hydrodenitrogention

Activity of Sulfided NiMo/Al_2O_3 Catalysts, *Catal. Today*, **292**, 58-66 (2017).

107. B. Caloch, M.S. Rana, J. Ancheyta, Improved Hydrogenolysis (C–S, C–M) Function with Basic Supported Hydrodesulfurization Catalysts, *Catal. Today*, **98**, 91-98 (2004).
108. H. Y. Zhu, N. Y. Shi, D. Y. Liu, R. Li, J. G. Yu, Q. T. Ma, ... & W. Y. Guo, New Insights into the Mechanism of Reactive Adsorption Desulfurization on Ni/ZnO Catalysts: Theoretical Evidence Showing the Existence of Interfacial Sulfur Transfer Pathway and the Essential Role of Hydrogen, *Petroleum Sci.*, **20**(5), 3240–3250 (2023).
109. F. Trejo, M.S. Rana, J. Ancheyta, CoMo/MgO–Al_2O_3 Supported Catalysts: An Alternative Approach to Prepare HDS Catalysts, *Catal. Today*, **130**, 327-336 (2008).
110. W. Chen, H. Nie, D. Li, X. Long, J. van Gestel, F. Maugé, Effect of Mg Addition on the Structure and Performance of Sulfide Mo/Al_2O_3 in HDS and HDN Reaction, *J. Catal.*, **344**, 420-433 (2016).
111. F. Rashidi, T. Sasaki, A.M. Rashidi, A.N. Kharat, K.J. Jozani, Ultradeep Hydrodesulfurization of Diesel Fuels Using Highly Efficient Nanoalumina-Supported Catalysts: Impact of Support, Phosphorus, and/or Boron on the Structure and Catalytic Activity, *J. Catal.*, **299**, 321-335 (2013).
112. O.V. Klimov, Y.V. Vatutina, K.A. Nadeina, M.O. Kazakov, E.Y. Gerasimov, I.P. Prosvirin, T.V. Larina, A.S. Noskov, CoMoB/Al_2O_3 Catalysts for Hydrotreating of Diesel Fuel. The Effect of the Way of the Boron Addition to a Support or an Impregnating Solution, *Catal. Today*, **305**, 192-202 (2018).
113. Y.V. Vatutina, O.V. Klimov, K.A. Nadeina, I.G. Danilova, E.Y. Gerasimov, I.P. Prosvirin, A.S. Noskov, Influence of Boron Addition to Alumina Support by Kneading on Morphology and Activity of HDS Catalysts, *Appl. Catal. B Environ.*, **199**, 23-32 (2016).
114. A. Haruna, et al., "Sulfur Removal Technologies from Fuel Oil for Safe and Sustainable Environment," *Fuel*, **329**, 125370 (2022).
115. W. Chen, F. Maugé, J. Van Gestel, H. Nie, D. Li, X. Long, Effect of Modification of the Alumina Acidity on the Properties of Supported Mo and CoMo Sulfide Catalysts, *J. Catal.*, **304**, 47-62 (2013).
116. O.V. Klimov, K.A. Nadeina, Y.V. Vatutina, E.A. Stolyarova, I.G. Danilova, E.Y. Gerasimov, I.P. Prosvirin, A.S. Noskov, CoMo/Al_2O_3 Hydrotreating Catalysts of Diesel Fuel with Improved Hydrodenitrogenation Activity, *Catal. Today*, **307**, 73-83 (2018).
117. R.L. Tong, Y.G. Wang, X. Zhang, H.Y. Zhang, J.Z. Dai, X.C. Lin, D.P. Xu, Effect of Phosphorus Modification on the Catalytic Properties of NiW/γ-Al_2O_3 in the Hydrogenation of Aromatics from Coal Tar, *J. Fuel Chem. Technol.*, **43**, 1461-1469 (2015).
118. A. García-Vila, R. Cuevas-García, J. Ramírez, I. Puente-Lee, Effect of Phosphorus on Mo/Al_2O_3 Catalysts for Maya Crude Improvement, *Catal. Today*, **220-222**, 310-317 (2014).
119. Z. Yu, X. Huang, S. Xun, M. He, L. Zhu, L. Wu, & H. Li, Synthesis of Carbon Nitride Supported Amphiphilic Phosphotungstic Acid Based Ionic Liquid for Deep Oxidative Desulfurization of Fuels, *J. Mol. Liq.*, **308**, 113059 (2020).
120. E. Altamirano, J.A. de Los Reyes, F. Murrieta, M. Vrinat, Hydrodesulfurization of 4,6-Dimethyldibenzothiophene over Co(Ni)MoS_2 Catalysts Supported on Alumina: Effect of Gallium as an Additive, *Catal. Today*, **133–135**, 292–298 (2008).
121. J.N. Díaz de León, M. Picquart, L. Massin, M. Vrinat, J.A. de los Reyes, Hydrodesulfurization of Sulfur Refractory Compounds: Effect of Gallium as an Additive in NiWS/γ-Al_2O_3 Catalysts, *J. Mol. Catal. A Chem.*, **363–364**, 311–321 (2012).
122. W. Zhou, Y. Zhang, X. Tao, Y. Zhou, Q. Wei, S. Ding, Effects of Gallium Addition to Mesoporous Alumina by Impregnation on Dibenzothiophene Hydrodesulfurization Performances of the Corresponding NiMo Supported Catalysts, *Fuel*, **228**, 152–163 (2018).
123. A. Olivas, P.A. Luque, C.M. Gómez-Gutierrez, D.L. Flores, R. Valdez, L. Escalante, P. Schacht, R. Silva-Rodrigo, Synthesis and Characterization of Mesoporous Supports Doped with NiW/Gax for Hydrodesulfurization of DBT, *Catal. Commun.*, **91**, 67–71 (2017).
124. W. Zhou, Q. Zhang, Y. Zhou, Q. Wei, L. Du, S. Ding, S. Jiang, Y. Zhang, Effects of Ga- and P-modified USY-based NiMoS Catalysts on Ultra-deep Hydrodesulfurization for FCC Diesels, *Catal. Today*, **305**, 171–181 (2018).
125. A. Maiello, Production of Adsorbents Derived from Nut Shells for H_2S Removal, (2022).
126. P.G. Moses, B. Hinnemann, H. Topsoe, J.K. Norskov, The Hydrogenation and Direct Desulfurization Reaction Pathway in Thiophene Hydrodesulfurization over MoS_2 Catalysts at Realistic Conditions: A Density Functional Study, *J. Catal.*, **248**, 188–203 (2007).
127. B. Yoosuk, C. Song, J.H. Kim, C. Ngamcharussrivichai, P. Prasassarakich, Effects of Preparation Conditions in Hydrothermal Synthesis of Highly Active Unsupported NiMo Sulfide Catalysts for Simultaneous Hydrodesulfurization of Dibenzothiophene and 4,6-Dimethyldibenzothiophene, *Catal. Today*, **149**, 52–61 (2010).

128. C. Fontaine, Y. Romero, A. Daudin, E. Devers, C. Bouchy, S. Brunet, Insight into Sulphur Compounds and Promoter Effects on Molybdenum-based Catalysts for Selective HDS of FCC Gasoline, *Appl. Catal. A Gen.*, **388**, 188–195 (2010).
129. F. Niefind, W. Bensch, M. Deng, L. Kienle, J.C. Reyes, D.V. Granados, Co-promoted MoS_2 for Hydrodesulfurization: New Preparation Method of MoS_2 at Room Temperature and Observation of Massive Differences of the Selectivity Depending on the Activation Atmosphere, *Appl. Catal. A Gen.*, **497**, 72–84 (2015).
130. B. S. Zhang, Y. J. Yi, W. Zhang, C. H. Liang, and D. S. Su, Electron Microscopy Investigation of the Microstructure of Unsupported Ni–Mo–W Sulfide, *Mater. Charact.*, **62**(7), 684–690 (2011).
131. R.H. Acuña, G.A. Nunez, F.P. Delgado, J.L. Romero, G. Berhault, E.M.R. Munoz, Unsupported Trimetallic CoMoW Sulfide HDS Catalysts Prepared by In Situ Decomposition of Sulfur-containing Precursors, *Catal. Today*, **250**, 28–37 (2015).
132. Y.E. Armenta, J.C. Reyes, F.P. Delgado, M.D. Valle, G. Alonso, S. Fuentes, R.R. Rivera, CoMoW Sulfide Nanocatalysts for the HDS of DBT from Novel Ammonium and Alkyltrimethylammonium-Thiomolybdate-Thiotungstate-Cobaltate (II) Precursors, *Appl. Catal. A Gen.*, **486**, 62–68 (2014).
133. L. Romero, M.D. Valle, R.R. Rivera, G. Alonso, M.A. Borja, S. Fuentes, F.P. Delgado, J.C. Reyesa, MoS_2 Catalysts Derived from N-Methylenediammonium Thiomolybdates During HDS of DBT, *Catal. Today*, **250**, 66–71 (2015).
134. Z. Le, P. Afanasiev, D. Li, Y. Shi, and M. Vrinat, Synthesis of Unsupported Ni–W–S Hydrotreating Catalysts from the Oxothiosalt $(NH_4)_2WO_2S_2$, *Compt. R. Chim.*, **11**(1–2), 130–136 (2008).
135. Y.G. Hur, D.W. Lee, K.Y. Lee, Hydrocracking of Vacuum Residue Using NiWS(x) Dispersed Catalysts, *Fuel*, **185**, 794-803 (2016).
136. T.C. Ho, J.M. McConnachie, Ultra-deep Hydrodesulfurization on MoS_2 and $Co0.1MoS_2$: Intrinsic vs. Environmental Factors, *J. Catal.*, **277**, 117–122 (2011).
137. A. Olivas, T.A. Zepeda, I. Villalpando, S. Fuentes, Performance of Unsupported Ni(Co,Fe)/MoS_2 Catalysts in Hydrotreating Reactions, *Catal. Commun.*, **9**, 1317–1328 (2008).
138. Y. Yi, B. Zhang, X. Jin, L. Wang, C.T. Williams, G. Xiong, D. Su, C. Liang, Unsupported NiMoW Sulfide Catalysts for Hydrodesulfurization of Dibenzothiophene by Thermal Decomposition of Thiosalts, *J. Mol. Catal. A Chem.*, **351**, 120–127 (2011).
139. J. Bocarando, R.H. Acuna, W. Bensch, Z.D. Huang, V. Petranovskii, S. Fuentes, G.A. Nunez, Unsupported Ni-Mo-W Sulphide HDS Catalysts with the Varying Nickel Concentration, *Appl. Catal. A Gen.*, **363**, 45–51 (2009).
140. T.A. Zepeda, B. Pawelec, J.N. Díaz de León, J.A. de los Reyes, A. Olivas, Effect of Gallium Loading on the Hydrodesulfurization Activity of Unsupported Ga_2S_3/WS_2 Catalysts, *Appl. Catal. B Environ.*, **111–112**, 10–19 (2012).
141. A. Daudin, A.F. Lamic, G. Perot, S. Brunet, P. Raybaud, C. Bouchy, Microkinetic Interpretation of HDS/HYDO Selectivity of the Transformation of a Model FCC Gasoline over Transition Metal Sulfides, *Catal. Today*, **130**, 221–230 (2008).
142. P. Afanasiev, The Influence of Reducing and Sulfiding Conditions on the Properties of Unsupported MoS_2-based Catalysts, *J. Catal.*, **269**, 269–280 (2010).
143. A. Daudin, A. F. Lamic, G. Perot, S. Brunet, P. Raybaud, and C. Bouchy, Microkinetic Interpretation of HDS/HYDO Selectivity of the Transformation of a Model FCC Gasoline over Transition Metal Sulfides, *Catal. Today*, **130**(1), 221–230 (2008).
144. T.L. Coelho, Y.E. Licea, L.A. Palacio, A.C. Faro Jr., Heptamolybdate-Intercalated CoMgAl Hydrotalcites as Precursors for HDS-Selective Hydrotreating Catalysts, *Catal. Today*, **250**, 38–46 (2015).
145. S.L. Amaya, G.A. Nunez, J.C. Reyes, S. Fuentes, A. Echavarria, Influence of the Sulfidation Temperature in a NiMoW Catalyst Derived from Layered Structure $(NH_4)Ni_2OH(H_2O)(MoO_4)_2$, *Fuel*, **139**, 575–583 (2015).
146. Y. Chen, L. Wang, Y. Zhang, T. Liu, X. Liu, Z. Jiang, C. Li, A New Multi-Metallic Bulk Catalyst with High Hydrodesulfurization Activity of 4,6-DMDBT Prepared Using Layered Hydroxide Salts as Structural Templates, *Appl. Catal. A Gen.*, **474**, 69–77 (2014).
147. C. Yin, Y. Wang, S. Xue, H. Liu, H. Li, C. Liu, Influence of Sulfidation Conditions on Morphology and Hydrotreating Performance of Unsupported Ni-Mo-W Catalysts, *Fuel*, **175**, 13–19 (2016).
148. H. Zhang, H. Lin, Y. Zheng, Y. Hu, A. MacLennan, Understanding of the Effect of Synthesis Temperature on the Crystallization and Activity of Nano-MoS_2 Catalyst, *Appl. Catal. B Environ.*, **165**, 537–546 (2015).
149. Y.C. Long, Z.X. Ping, Z.L. Yyan, L.C. Guang, Mechanism of Hydrodesulfurization of Dibenzothiophenes on Unsupported NiMoW Catalyst, *J. Fuel Chem. Technol.*, **41**, 991–997 (2013).
150. C. Liu, H. Liu, C. Yin, X. Zhao, B. Liu, X. Li, Y. Li, Y. Liu, Preparation, Characterization, and Hydrodesulfurization Properties of Binary Transition-Metal Sulfide Catalysts, *Fuel*, **154**, 88–94 (2015).

151. C. Yin, L. Zhao, Z. Bai, H. Liu, Y. Liu, C. Liu, A Novel Porous Ammonium Nickel Molybdate as the Catalyst Precursor Towards Deep Hydrodesulfurization of Gas Oil, *Fuel*, **107**, 873–878 (2013).
152. P. Li, Y. Chen, C. Zhang, B. Huang, X. Liu, T. Liu, Z. Jiang, C. Li, Highly Selective Hydrodesulfurization of Gasoline on Unsupported Co-Mo Sulfide Catalysts: Effect of MoS_2 Morphology, *Appl. Catal. A Gen.*, **533**, 99–108 (2017).
153. E. Blanco, D. Uzio, G. Berhault, P. Afanasiev, From Core–Shell MoSx/ZnS to Open Fullerene-Like MoS_2 Nanoparticles, *J. Mater. Chem.*, **2**, 3325–3331 (2014).
154. A.H. Aissa, F. Dassenoy, C. Geantet, P. Afanasiev, Solution Synthesis of Core–Shell Co_9S_8@MoS_2 Catalysts, *Catal. Sci. Technol.*, **6**, 4901–4909 (2016).
155. Li Yue, et al., Size-Dependent Activity of Unsupported Co–Mo Sulfide Catalysts for the Hydrodesulfurization of Dibenzothiophene, *Appl. Catal. A Gen.*, **512**, 85–92 (2016).
156. A. Mansouri, N. Semagina, Promotion of Niobium Oxide Sulfidation by Copper and Its Effects on Hydrodesulfurization Catalysis, *ACS Catal.*, **8**, 7621–7632 (2018).
157. Z. Le, L. Xiangyun, L. Dadong, G. Xiaodong, Study on High-Performance Unsupported Ni–Mo–W Hydrotreating Catalyst, *Catal. Commun.*, **12**, 927–931 (2011).
158. P. Afanasiev, C. Geantet, I. Llorens, and O. Proux, Biotemplated Synthesis of Highly Divided MoS_2 Catalysts, *J. Mater. Chem.*, **22**(19), 9731–9737 (2012).
159. C. Zhang, P. Li, X. Liu, T. Liu, Z. Jiang, C. Li, Morphology-Performance Relation of (Co)MoS_2 Catalysts in the Hydrodesulfurization of FCC Gasoline, *Appl. Catal. A Gen.*, **556**, 20–28 (2018).
160. J. Gusakova, X. Wang, L. Lynn Shiau, A. Krivosheeva, V. Shaposhnikov, V. Borisenko, V. Gusakov, B. Kang Tay, Electronic Properties of Bulk and Monolayer TMDs: Theoretical Study Within DFT Framework (GVJ-2e Method), *Phys. Status Solidi*, **214**, 1700218 (2017).
161. S.S. Coutinho, M.S. Tavares, C.A. Barboza, N.F. Frazão, E. Moreira, D.L. Azevedo, 3R and 2H Polytypes of MoS_2: DFT and DFPT Calculations of Structural, Optoelectronic, Vibrational and Thermodynamic Properties, *J. Phys. Chem. Solids*, **111**, 25–33 (2017).
162. V.V. Ivanovskaya, A. Zobelli, A. Gloter, N. Brun, V. Serin, C. Colliex, "Ab Initio Study of Bilateral Doping Within the MoS_2-NbS_2 System," *Phys. Rev. B*, 78, 134104 (2008).
163. J. Suh, T. Leong Tan, W. Zhao, J. Park, D.-Y. Lin, T.-E. Park, J. Kim, C. Jin, N. Saigal, S. Ghosh, et al., Reconfiguring Crystal and Electronic Structures of MoS_2 by Substitutional Doping, *Nat. Commun.*, 9, **199** (2018).
164. M. Brotons-Gisbert, A. Segura, R. Robles, E. Canadell, P. Ordejón, J.F. Sánchez-Royo, Optical and Electronic Properties of 2H−MoS_2 Under Pressure: Revealing the Spin-Polarized Nature of Bulk Electronic Bands, *Phys. Rev. Mater.*, **2**, 054602 (2018).
165. W. Zhou, X. Zou, S. Najmaei, Z. Liu, Y. Shi, J. Kong, J. Lou, P.M. Ajayan, B.I. Yakobson, J.-C. Idrobo, Intrinsic Structural Defects in Monolayer Molybdenum Disulfide, *Nano Lett.*, **13**, 2615–2622 (2013).
166. H. Wan, L. Xu, W.Q. Huang, J.H. Zhou, C.N. He, X. Li, G.F. Huang, P. Peng, Z.G. Zhou, Band Structure Engineering of Monolayer MoS_2: A Charge Compensated Codoping Strategy, *RSC Adv.*, **5**, 7944–7952 (2015).
167. Q. Tang, D.E. Jiang, Stabilization and Band-Gap Tuning of the 1T-MoS_2 Monolayer by Covalent Functionalization, *Chem. Mater.*, **27**, 3743–3748 (2015).
168. A.V. Krivosheeva, V.L. Shaposhnikov, V.E. Borisenko, J.L. Lazzari, W.C. Waileong, J. Gusakova, B.K. Tay, Theoretical Study of Defect Impact on Two-Dimensional MoS_2, *J. Semicond.*, **36**, 122002 (2015).
169. C. Li, B. Fan, W. Li, L. Wen, Y. Liu, T. Wang, K. Sheng, Y. Yin, Bandgap Engineering of Monolayer MoS_2 Under Strain: A DFT Study, *J. Korean Phys. Soc.*, **66**, 1789–1793 (2015).
170. T. Li, G. Galli, Electronic Properties of MoS_2 Nanoparticles, *J. Phys. Chem. C*, **111(44)**, 16192-16196 (2007).
171. M.V. Bollinger, K.W. Jacobsen, J.K. Nørskov, Atomic and Electronic Structure of MoS_2 Nanoparticles, *Phys. Rev. B Condens. Matter Mater. Phys.*, **67**, 085410 (2003).
172. M. Javaid, D.W. Drumm, S.P. Russo, A.D. Greentree, A Study of Size-Dependent Properties of MoS_2 Monolayer Nanoflakes Using Density-Functional Theory, *Sci. Rep.*, **7**, 9775 (2017).
173. X. Liu, D. Cao, T. Yang, H. Li, H. Ge, M. Ramos, Q. Peng, A.K. Dearden, Z. Cao, Y. Yang, et al., Insight into the Structure and Energy of $Mo_{27}S_xO_y$clusters, *RSC Adv.*, **7**, 9513–9520 (2017).
174. N. Li, G. Lee, Y.H. Jeong, K.S. Kim, Tailoring Electronic and Magnetic Properties of MoS_2 Nanotubes, *J. Phys. Chem. C*, **119**, 6405–6413 (2015).
175. R. Wang, H. Sun, B. Ma, J. Hu, J. Pan, Edge Passivation Induced Single-Edge Ferromagnetism of Zigzag MoS_2 Nanoribbons, *Phys. Lett. A*, **381**, 301–306 (2017).

176. Y. Li, Z. Zhou, S. Zhang, Z. Chen, MoS_2 Nanoribbons: High Stability and Unusual Electronic and Magnetic Properties, *J. Am. Chem. Soc*., **130**, 16739–16744 (2008).
177. P. Raybaud, J. Hafner, G. Kresse, S. Kasztelan, H. Toulhoat, Ab Initio Study of the H_2–H_2S/MoS_2 Gas–Solid Interface: The Nature of the Catalytically Active Sites, *J. Catal.*, **189**, 129–146 (2000).
178. S. Li, Y. Liu, Z. Feng, X. Chen, C. Yang, Insights into the Reaction Pathway of Thiophene Hydrodesulfurization over Corner Site of MoS_2 Catalyst: A Density Functional Theory Study, *Mol. Catal.*, **463**, 45–63 (2019).
179. J. Bonde, P.G. Moses, T.F. Jaramillo, J.K. Nørskov, I. Chorkendorff, Hydrogen Evolution on Nano-Particle Transition Metal Sulfides, *Faraday Discuss.*, **140**, 219–231 (2009).
180. H. Wang, C. Tsai, D. Kong, K. Chan, F. Abild-Pedersen, J.K. Nørskov, Y. Cui, Transition-Metal Doped Edge Sites in Vertically Aligned MoS_2 Catalysts for Enhanced Hydrogen Evolution, *Nano Res.*, **8**, 566–575 (2015).
181. Q. Jin, B. Chen, Z. Ren, X. Liang, N. Liu, D. Mei, A Theoretical Study on Reaction Mechanisms and Kinetics of Thiophene Hydrodesulfurization over MoS_2 Catalysts, *Catal. Today*, **312**, 158–167 (2018).
182. A.M. Silva, I. Borges, how to Find an Optimum Cluster Size Through Topological Site Properties: MoSx Model Clusters, *J. Comput. Chem.*, **32**, 2186–2194 (2011).
183. T. Yang, J. Feng, X. Liu, Y. Wang, H. Ge, D. Cao, & B. Shen, A Combined Computational and Experimental Study of the Adsorption of Sulfur Containing Molecules on Molybdenum Disulfide Nanoparticles, *J. Mater. Res.*, **33**(21), 3589–3603 (2018).
184. S.S. Gronborg, M. Saric, P.G. Moses, J. Rossmeisl, J.V. Lauritsen, Atomic Scale Analysis of Sterical Effects in the Adsorption of 4,6-Dimethyldibenzothiophene on a CoMoS Hydrotreating Catalyst, *J. Catal.*, **344**, 121–128 (2016).
185. S.S. Gronborg, M. Saric, P.G. Moses, J. Rossmeisl, J.V. Lauritsen, Atomic Scale Analysis of Sterical Effects in the Adsorption of 4,6-Dimethyldibenzothiophene on a CoMoS Hydrotreating Catalyst, *J. Catal.*, **344**, 121–128 (2016).
186. B. Hinnemann, J.K. Nørskov, H. Topsøe, A Density Functional Study of the Chemical Differences Between Type I and Type II MoS_2-Based Structures in Hydrotreating Catalysts, *J. Phys. Chem. B*, **109**, 2245–2253 (2005).
187. H. Topsøe, B. Hinnemann, J. K. Nørskov, J. V. Lauritsen, F. Besenbacher, P. L. Hansen, & K. G. Knudsen, The Role of Reaction Pathways and Support Interactions in the Development of High Activity Hydrotreating Catalysts, *Catal. Today*, **107**, 12–22 (2005).
188. E. Krebs, A. Daudin, and P. Raybaud, A DFT Study of CoMoS and NiMoS Catalysts: From Nano-Crystallite Morphology to Selective Hydrodesulfurization, *Oil Gas Sci. Technol. IFP*, **64**, 707–718 (2009).
189. M. Badawi, J. Paul, E. Payen, Y. Romero, F. Richard, S. Brunet, A. Popov, E. Kondratieva, J. Gilson, L. Mariey, Hydrodeoxygenation of Phenolic Compounds by Sulfided (Co)Mo/Al_2O_3 Catalysts: A Combined Experimental and Theoretical Study, *Oil Gas Sci. Technol.*, **68**, 829–840 (2013).
190. I. Czekaj, J. Wambach, O. Kröcher, Modelling Catalyst Surfaces Using DFT Cluster Calculations, *Int. J. Mol. Sci.*, **10**, 4310–4329 (2009).
191. B. Hinnemann, J. Nørskov, H. Topsøe, A Density Functional Study of the Chemical Differences Between Type I and Type II MoS_2-Based Structures in Hydrotreating Catalysts, *J. Phys. Chem. B*, **109**, 2245–2253 (2005).
192. H. Topsøe, B. Hinnemann, J. Nørskov, J. Lauritsen, F. Besenbacher, P. Hansen, G. Hytoft, R. Egeberg, K. Knudsen, The Role of Reaction Pathways and Support Interactions in the Development of High Activity Hydrotreating Catalysts, *Catal. Today*, **107–108**, 12–22 (2005).
193. S. Kolboe, Catalytic Hydrodesulfurization of Thiophene. VII. Comparison Between Thiophene, Tetrahydrothiophene, and *n*-Butanethiol, *Can. J. Chem.*, **47**, 352–355 (1969).
194. J.G. Lipsch,.C.A. Schuit, The CoO-MoO_3-Al_2O_3 Catalyst: III. Catalytic Properties, *J. Catal.*, **15**, 179–189 (1969).
195. J. Kraus, M. Zdrazil, *React. Kinet. Catal. Lett.*, **6**, 475 (1977).
196. J. Devanneaux, J. Maurin, Hydrogenolysis and Hydrogenation of Thiophenic Compounds on a Co-Mo/Al_2O_3 Catalyst, *J. Catal.*, **69**, 1 (1981).
197. B.T. Carvill, L.T. Thompson, Hydrodesulfurization Over Model Sulfide Cluster-Derived Catalysts, *Appl. Catal.*, **75**, 249–265 (1991).
198. E. J. Markel, G. L. Schrader, N. N. Sauer, and R. J. Angelici, Thiophene, 2,3- and 2,5-Dihydrothiophene, and Tetrahydrothiophene Hydrodesulfurization on Mo and Re/γ-Al_2O_3 Catalysts, *J. Catal.*, **116**(1), 11–22 (1989).
199. J. P. Vissers, C. K. Groot, E. M. Van Oers, D. Beer, and R. Prins, Carbon-Supported Transition Metal Sulfides, *Bull. Soc. Chim. Belg.*, **93**(8-9), 813–822 (1984).
200. T.A. Pecoraro, R.R. Chianelli, Hydrodesulfurization Catalysis by Transition Metal Sulfides, *J. Catal.*, **67**, 430–445 (1981).

201. M. J. Ledoux, O. Michaux, G. Agostini, and P. Panissod, The Influence of Sulfide Structures on the Hydrodesulfurization Activity of Carbon-Supported Catalysts, *J. Catal.*, **102**(2), 275–288 (1986).
202. S. Harris, R.R. Chianelli, Catalysis by Transition Metal Sulfides: The Relation Between Calculated Electronic Trends and HDS Activity, *J. Catal.*, **86**, 400–412 (1984).
203. J.K. Nørskov, B.S. Clausen, H. Topsøe, Understanding the Trends in the Hydrodesulfurization Activity of the Transition Metal Sulfides, *Catal. Lett.*, **13**, 1–8 (1992).
204. B.C. Wiegand, C.M. Friend, Model Studies of the Desulfurization Reactions on Metal Surfaces and in Organometallic Complexes, *Chem. Rev.*, **92**, 491–504 (1998).
205. T.S. Smit, K.H. Johnson, A Unified Theory of Periodic and Promotion Effects in Transition Metal Sulfide Hydrodesulfurization Catalysts, *Catal. Lett.*, **28**, 361 (2010).
206. H. Topsøe, B. S. Clausen, R. Candia, C. Wivel, and S. Mørup, *In situ* Mössbauer Emission Spectroscopy Studies of Unsupported and Supported Sulfided Co-Mo Hydrodesulfurization Catalysts: Evidence for and Nature of a Co-Mo-S Phase, *J. Catal.*, **68**, 433 (2020).
207. B. Delmon, "A New Hypothesis Explaining Synergy Between Two Phases in Heterogeneous Catalysis: The Case of Hydrodesulfurization Catalysts," *Bull. Soc. Chim. Belg.*, **88**, 979 (2019).
208. H. Topsøe, B. S. Clausen, R. Candia, C. Wivel, and S. Mørup, *In situ* Mössbauer Emission Spectroscopy Studies of Unsupported and Supported Sulfided Co-Mo Hydrodesulfurization Catalysts: Evidence for and Nature of a Co-Mo-S Phase, *J. Catal.*, **68**, 433 (2020).
209. B. Delmon, A New Hypothesis Explaining Synergy Between Two Phases in Heterogeneous Catalysis: The Case of Hydrodesulfurization Catalysts, *Bull. Soc. Chim. Belg.*, **88**, 979 (2019).
210. M. Daage, R.R. Chianelli, Structure-Function Relations in Molybdenum Sulfide Catalysts: The 'Rim-Edge' Model, *J. Catal.*, **149**, 414 (2018).
211. V.H. De Beer, J.C. Duchet, R. Prins, The Role of Cobalt and Nickel in Hydrodesulfurization: Promoters or Catalysts, *J. Catal.*, **72**, 369 (2020).
212. J. C. Duchet, E. M. Van Oers, V. H. De Beer, and R. Prins, Carbon-Supported Sulfide Catalysts, *J. Catal.*, **80**, 386 (1983).
213. W. J. Crajé, V. H. De Beer and A. M. Van der Kraan, On the So-Called Co-Mo-S Phase Observed in Carbon-Supported Cobalt Sulfide Catalysts: Temperature Dependence of the In-Situ Mössbauer Emission Spectrum, *Appl. Catal.*, **70**, L7 (1991).
214. M. W. Crajé, V. H. De Beer, J. A. Van Veen, and A. M. Van der Kraan, On the Identification of "Co-Sulfide" Species in Sulfided Supported Co and CoMo Catalysts, *Chem. Ind. New York Marcel Dekker*, 95–114 (1996).
215. A. Haruna, et al., "Sulfur Removal Technologies from Fuel Oil for Safe and Sustainable Environment," *Fuel*, **329**, 125370 (2022).
216. X. Li, X. Yang, J. Zhang, Y. Huang, and B. Liu, In Situ/Operando Techniques for Characterization of Single-Atom Catalysts, *ACS Catal.*, **9**(3), 2521–2531 (2019).
217. C. Barroo, Z. J. Wang, R. Schlögl, and M. G. Willinger, Imaging the Dynamics of Catalysed Surface Reactions by In Situ Scanning Electron Microscopy, *Nat. Catal.*, **3**(1), 30–39 (2020).
218. E. D. Boyes and P. L. Gai, Environmental High Resolution Electron Microscopy and Applications to Chemical Science, *Ultramicroscopy*, **67**, 219 (1997).
219. H. Y. Chao, K. Venkatraman, S. Moniri, Y. Jiang, X. Tang, S. Dai, and M. Chi, In Situ and Emerging Transmission Electron Microscopy for Catalysis Research, *Chem. Rev.*, **123**(13), 8347–8394 (2023).
220. R. Hu, Y. Liu, S. Shin, S. Huang, X. Ren, W. Shu, and X. Luo, Emerging Materials and Strategies for Personal Thermal Management, *Adv. Energy Mater.*, **10**(17), 1903921 (2020).
221. F. M. Ross, Opportunities and Challenges in Liquid Cell Electron Microscopy, *Science*, **350**, 9886 (2015).
222. C. Ophus, Four-Dimensional Scanning Transmission Electron Microscopy (4D-STEM): From Scanning Nanodiffraction to Ptychography and Beyond, *Microsc. Microanal.*, **25**, 563–582 (2019).
223. Y. Yang, S. Louisia, S. Yu, J. Jin, I. Roh, C. Chen, and P. Yang, Operando Studies Reveal Active Cu Nanograins for CO_2 Electroreduction, *Nature*, **614**(7947), 262–269 (2023).